



THE UNIVERSITY OF
WAIKATO
Te Whare Wānanga o Waikato

Research Commons

<http://waikato.researchgateway.ac.nz/>

Research Commons at the University of Waikato

Copyright Statement:

The digital copy of this thesis is protected by the Copyright Act 1994 (New Zealand).

The thesis may be consulted by you, provided you comply with the provisions of the Act and the following conditions of use:

- Any use you make of these documents or images must be for research or private study purposes only, and you may not make them available to any other person.
- Authors control the copyright of their thesis. You will recognise the author's right to be identified as the author of the thesis, and due acknowledgement will be made to the author where appropriate.
- You will obtain the author's permission before publishing any material from the thesis.

Rediscovering Arsenoacetic Acid

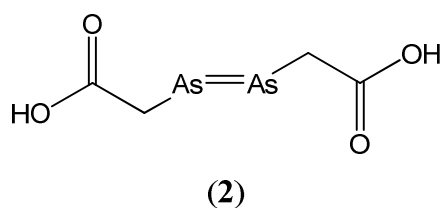
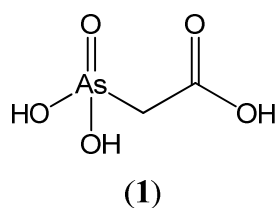


THE UNIVERSITY OF
WAIKATO
Te Whare Wānanga o Waikato

A thesis
submitted in partial fulfilment
of the requirements for the degree
of
Master of Science in Chemistry
at
The University of Waikato
by
Peter Stanley Wilson

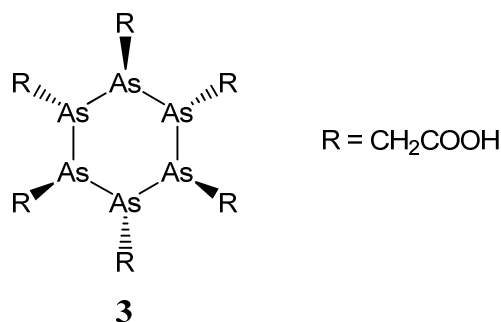
Abstract

Arsonoacetic acid, $\text{H}_2\text{O}_3\text{As}^{\text{I}}\text{CH}_2\text{COOH}$ (**1**), and arsenoacetic acid, punitively $[\text{As}^{\text{V}}\text{CH}_2\text{COOH}]_2$ (**2**) have been synthesised according to historical literature methods, and have been characterised using modern techniques.



Arsonoacetic acid was shown by an X-ray crystal structure analysis to be a molecular species with an extensive hydrogen bonding network in the crystal.

Arsenoacetic acid proved to be more enigmatic. Electrospray mass spectra suggested it consisted of a mixtures of rings $(\text{RAs})_n$, $n = 3-11$, with $n = 6$ dominating. This was partly confirmed by a crystal structure of $(\text{AsCH}_2\text{COOH})_6$ (**3**) (as the pyridine solvate). On the other hand, ^1H and ^{13}C NMR gave spectra that indicated only a single component for arsenoacetic acid.



The formation of crystals of the high temperature phase of elemental sulfur, $\beta\text{-S}_8$, at ambient temperature is also discussed.

Acknowledgements

Firstly, I would like to thank my supervisor Professor Brian Nicholson for his guidance throughout the last two years and helping me make sense of my many 'interesting' results, why nothing was simple and straight forward is beyond me. Your input into this thesis right up until the last minute is greatly appreciated.

Thank you to all my fellow students that entertained me and helped me through this time. Special thanks to Kelly for her expertise in NMR, Bevan for his flawless logic, and Leah for her shared interest in caffeinated beverages that kept us going. Huge thanks to Simon, after 12 years of academic rivalry, it is now time to part ways and I wish you all the best.

To my friends who have kept me sane, and kept things in perspective, thank you for your patience, reassurance and timely distractions.

And last but not least, a resounding thank you my family. Thanks Emma and Ryan for a place to chill out, and for your impeccable taste in comedy. Mum and Dad, thank you, thank you, thank you, for your unceasing support and encouragement and a place to always call home.

Table of Contents

Abstract.....	ii
Acknowledgements	iii
Table of Contents.....	iv
List of Figures	vi
List of Tables	viii
List of Abbreviations	x
1. Introduction.....	1
1.1 <i>Medicinal arsenic</i>	1
1.1.1 Salvarsan	3
1.1.2 The arsenic eaters of Styria.....	4
1.2 <i>The toxicity of arsenic</i>	5
1.3 <i>Uses of arsenic</i>	7
1.4 <i>Preparations of arsonic acids and arseno compounds</i>	8
1.4.1 Arsonic acids.....	8
1.4.2 Arseno compounds	9
1.5 <i>Usage and history of arsono- and arsenoacetic acid</i>	9
1.5.1 Arsonoacetic acid.....	9
1.5.2 Arsenoacetic acid.....	10
1.6 <i>X-ray crystallography</i>	11
2. Experimental.....	12
2.1 <i>General</i>	12
2.2 <i>Instrumental techniques</i>	12
2.2.1 EDX spectroscopy	12
2.2.2 FT-IR spectroscopy	12
2.2.3 GC-MS.....	12
2.2.4 High-resolution mass spectrometry	12
2.2.5 HPLC	13
2.2.6 NMR spectroscopy	13
2.3 <i>Synthesis of barium arsonoacetic acid – (BaO₃AsCH₂COO)₂Ba</i>	13

2.4	Synthesis of sodium arsonoacetic acid – $\text{Na}_2\text{O}_3\text{AsCH}_2\text{COONa}\cdot\text{H}_2\text{O}$	14
2.5	Synthesis of arsonoacetic acid – $\text{H}_2\text{O}_3\text{AsCH}_2\text{COOH}$	15
2.6	X-ray crystal structure of arsonoacetic acid – $\text{H}_2\text{O}_3\text{AsCH}_2\text{COOH}$	16
2.7	Synthesis of arsenoacetic acid – $\text{As}_x(\text{CH}_2\text{COOH})_x$	17
2.8	X-ray crystal structure of cyclohexaarsenoacetic acid – $\text{As}_6(\text{CH}_2\text{COOH})_6\cdot 6\text{C}_5\text{NH}_5$	18
2.9	Synthesis of sodium arsenoacetic acid – $\text{As}_x(\text{CH}_2\text{COONa})_x$	19
2.10	Attempted esterification of arsenoacetic acid – $(\text{AsCH}_2\text{COOCH}_3)_x$	20
2.11	X-ray crystal structure of S_8	20
3.	Results and Discussion	21
3.1	Arsonoacetic acid and its salts.....	21
3.1.1	Synthesis.....	21
3.1.2	EDX analysis of barium arsonoacetic acid.....	22
3.1.3	Discussion of X-ray crystal structure of arsonoacetic acid	22
3.1.4	Discussion of FT-IR results.....	25
3.1.5	Discussion of HRMS results.....	27
3.1.6	Discussion of NMR results	30
3.2	Arsenoacetic acid	32
3.2.1	Synthesis.....	32
3.2.2	Discussion of X-ray crystal structure of cyclohexaarsenoacetic acid.....	33
3.2.3	Discussion of FT-IR results.....	37
3.2.4	Discussion of HRMS results.....	38
3.2.5	Discussion of NMR results	42
3.2.6	Attempted separation of rings using HPLC.....	45
3.2.7	Attempted esterification of arsenoacetic acid, NMR spectroscopy and GC-MS results	48
3.2.8	Discussion of X-ray crystal structure of β -monoclinic S_8 (β - S_8)	50
4.	Conclusions	53
5.	Appendix – Complete X-Ray Crystal Data	54
5.1	Arsonoacetic acid – $\text{H}_2\text{O}_3\text{AsCH}_2\text{COOH}$	54
5.2	Cyclohexaarsenoacetic acid – $\text{As}_6(\text{CH}_2\text{COOH})_6\cdot 6\text{C}_5\text{NH}_5$	58
5.3	β -Monoclinic S_8 (β - S_8).....	67
6.	References.....	72

List of Figures

Figure 1.1 – Structure of Melarsaprol (Mel B), used to treat African sleeping sickness.....	2
Figure 1.2 – (a) Ehrlich’s proposed structure of Salvarsan, (b) main constituents of Salvarsan as published by Lloyd <i>et al.</i> ¹⁷	3
Figure 1.3 – Arsenic and arsenous acid and their methylated derivatives.....	5
Figure 1.4 – Palmer’s proposed structure of arsenoacetic acid.....	10
Figure 3.1 – Reaction scheme for arsonoacetic acid.....	21
Figure 3.2 – The structure and labelling scheme of arsonoacetic acid.....	22
Figure 3.3 – Crystal packing diagram of arsonoacetic acid showing intermolecular hydrogen bonding	24
Figure 3.4 – FT-IR spectra of (1) arsonoacetic acid, (2) sodium arsonoacetic acid, (3) barium arsonoacetic acid, KBr disc.....	25
Figure 3.5 – HRMS of arsonoacetic acid in H ₂ O, negative ion mode	27
Figure 3.6 – Scheme for the formation of the peak at <i>m/z</i> 348.86 in the HRMS spectrum of arsonoacetic acid (Figure 3.5)	27
Figure 3.7 – Structure of a phosphonium ylide and its resonance phosphorane form.....	28
Figure 3.8 – Proposed structure of 260.877 Da ion in arsonoacetic acid mass spectrum...	28
Figure 3.9 – HRMS of sodium arsonoacetic acid in H ₂ O, negative ion mode	29
Figure 3.10 – ¹ H NMR of the sodium salt and free acid of arsonoacetic acid (D ₂ O)	30
Figure 3.11 – ¹³ C NMR of sodium salt and free acid of arsonoacetic acid (D ₂ O).....	31
Figure 3.12 – Reaction scheme for arsenoacetic acid	32
Figure 3.13 – The structure and labelling scheme of cyclohexaarsenoacetic acid (pyridine solvate molecules omitted for clarity)	33
Figure 3.14 – Structure of cyclohexaarsonoacetic acid with the six hydrogen bonded pyridine solvate molecules.....	35
Figure 3.15 – Crystal packing diagram of cyclohexaarsenoacetic acid showing hydrogen bonds to pyridine molecules	35
Figure 3.16 – Structural diagram showing the stacking of a layer of pyridine molecules in the cyclohexaarsenoacetic acid crystal structure	36

Figure 3.17 – FT-IR spectrum of (1) arsenoacetic acid, (2) arsonoacetic acid	37
Figure 3.18 – Diagram showing (a) Palmer’s original diarsene structure of arsenoacetic acid, (b) newly proposed cyclic structure	38
Figure 3.19 – HRMS of arsenoacetic acid in H ₂ O, <i>m/z</i> 400-850, negative ion mode.....	39
Figure 3.20 – HRMS of sodium arsenoacetic acid in H ₂ O, negative ion mode.....	40
Figure 3.21 – Isotope patterns of the 422.788 and 400.806 Da ions in the sodium arsonoacetic acid mass spectrum.....	41
Figure 3.22 – ¹³ C NMR data comparing arsenoacetic (pyridine- <i>d</i> ₅) and its precursor arsonoacetic acid (D ₂ O)	43
Figure 3.23 – ¹ H NMR spectrum of arsenoacetic acid (pyridine- <i>d</i> ₅) with expansion and resolution enhancement of CH ₂ peak	44
Figure 3.24 – ¹³ C NMR spectrum of arsenoacetic acid (pyridine- <i>d</i> ₅) with expansion and resolution enhancement of CH ₂ peak	44
Figure 3.25 – HPLC max plot of arsenoacetic acid in 5:95 MeCN:H ₂ O, 50 mmol NaOH (190 – 400 nm).....	46
Figure 3.26 – HPLC max plot of arsenoacetic acid in 5:95 MeCN:H ₂ O, 40 mmol pyridine (190 – 400 nm)	47
Figure 3.27 – ¹ H NMR of crude solution from attempted esterification of arsenoacetic acid (CDCl ₃)	49
Figure 3.28 – TIC from GC-MS of crude methanol solution from the esterification of arsenoacetic acid.....	50
Figure 3.29 – Molecular diagram of β-monoclinic S ₈ showing unit cell and labelling scheme	51

List of Tables

Table 2.1 – HRMS data for sodium arsonoacetic acid, where $R = \text{CH}_2\text{COO}^-$	15
Table 2.2 – HRMS data for arsonoacetic acid – $\text{H}_2\text{O}_3\text{AsCH}_2\text{COOH}$	16
Table 2.3 – HRMS data for arsonoacetic acid – As_xR_x , where $R = \text{CH}_2\text{COOH}$	17
Table 2.4 – Selected HRMS data for sodium arsonoacetic acid, where $R = \text{CH}_2\text{COOH}$	19
Table 3.1 – Selected bond lengths (Å) comparing arsono- and phosphono- acetic acid	23
Table 3.2 – Hydrogen bonds for arsonoacetic acid (Å and °)	24
Table 3.3 – Summary and comparison of FT-IR data for the barium salt, sodium salt and free acid of arsonoacetic acid (cm^{-1})	26
Table 3.4 – Selected bond lengths and angles for cyclohexaarsenoacetic acid	34
Table 3.5 – Hydrogen bonds for cyclohexaarsenoacetic acid (Å and °)	36
Table 3.6 – Summary and comparison of FT-IR data for arsono- acid and arsono- acetic acid (cm^{-1})	38
Table 3.7 – Peak assignment for the HRMS of sodium arsonoacetic acid (Figure 3.20)	41
Table 5.1 – Crystal data and structure refinement for arsonoacetic acid	54
Table 5.2 – Atomic coordinates ($\times 10^4$) and equivalent isotropic displacement parameters ($\text{\AA}^2 \times 10^3$) for arsonoacetic acid	55
Table 5.3 – Complete bond lengths (Å) for arsonoacetic acid	55
Table 5.4 – Complete bond angles (°) for arsonoacetic acid	55
Table 5.5 – Anisotropic displacement parameters ($\text{\AA}^2 \times 10^3$) for arsonoacetic acid	56
Table 5.6 – Hydrogen coordinates ($\times 10^4$) and isotropic displacement parameters ($\text{\AA}^2 \times 10^3$) for arsonoacetic acid	56
Table 5.7 – Torsion angles (°) for arsonoacetic acid	56
Table 5.8 – Hydrogen bonds for arsonoacetic acid (Å and °)	57
Table 5.9 – Complete crystal data and structure refinement for arsonoacetic acid	58
Table 5.10 – Atomic coordinates ($\times 10^4$) and equivalent isotropic displacement parameters ($\text{\AA}^2 \times 10^3$) for arsonoacetic acid	59
Table 5.11 – Complete bond lengths (Å) for arsonoacetic acid	60

Table 5.12 – Complete bond angles (°) for arsenoacetic acid	61
Table 5.13 – Anisotropic displacement parameters ($\text{\AA}^2 \times 10^3$) for arsenoacetic acid	62
Table 5.14 – Hydrogen coordinates ($\times 10^4$) and isotropic displacement parameters ($\text{\AA}^2 \times 10^3$) for arsenoacetic acid	64
Table 5.15 – Torsion angles (°) for arsenoacetic acid	65
Table 5.16 – Hydrogen bonds for arsenoacetic acid (\AA and °)	66
Table 5.17 – Crystal data and structure refinement for β -S ₈	67
Table 5.18 – Atomic coordinates ($\times 10^4$) and equivalent isotropic displacement parameters ($\text{\AA}^2 \times 10^3$) for β -S ₈	68
Table 5.19 – Bond lengths (\AA) for β -S ₈	69
Table 5.20 – Bond angles (°) for β -S ₈	69
Table 5.21 – Anisotropic displacement parameters ($\text{\AA}^2 \times 10^3$) for β -S ₈	70
Table 5.22 – Torsion angles (°) for β -S ₈	71

List of Abbreviations

EDX	Energy-Dispersive X-Ray Spectroscopy
EI	Electron Impact
ESI	Electrospray Ionisation
FT-IR	Fourier Transform - Infrared
GC-MS	Gas Chromatography – Mass Spectrometry
HPLC	High Performance Liquid Chromatography
HRMS	High Resolution Mass Spectrometry
NMR	Nuclear Magnetic Resonance
PDA	Photodiode Array
SEM	Scanning Electron Microscope
TIC	Total Ion Chromatogram
TOF	Time of Flight
UV-Vis	Ultraviolet - Visible

1. Introduction

The history of arsenic is colourful, and its uses have varied from chemical weapons, to beauty products. A recent review of the diverse nature of arsenic, and the role it has played in many aspects of society has been written by Cullen,¹ and has been a basis for much of the introduction of this thesis.

1.1 Medicinal arsenic

Arsenic has been widely used therapeutically for the better part of the last 2400 years despite its high toxicity.^{2, 3} One of the first recorded uses of arsenic medicinally goes as far back as 400 BC when Hippocrates (460 - 370 BC) used the arsenic containing minerals, orpiment (As_2S_3) and realgar (As_2S_2), to treat tumours and cancerous ulcers. Reference to these same minerals was also found in ancient Chinese and Indian medicinal texts, dating back to 200 BC.⁴⁻⁶ Even though the use of these minerals were documented across the globe, arsenic itself had not yet been isolated or identified. It appears the first person to isolate arsenic, although disputed, was Saint Albert the Great (Albert Magnus) in 1205 AD.^{5, 7}

By the 18th century, people had been convinced that arsenic, although highly toxic, could be used therapeutically when the dosage was right, leading to the prescription of arsenic based drugs to cure a wide range of ailments. Paracelsus (1493 – 1541), an alchemist and physician, is quoted, “All substances are poisons; there is none which is not a poison. The right dose differentiates a poison and a remedy.”⁸ Fowler’s solution, a 1% solution of potassium arsenite, was a tonic readily prescribed for over 150 years as a cure for asthma, eczema, Hodgkin’s disease, anaemia, rheumatism and psoriasis, apparently with much success.^{3, 9} Patients would take 12 drops, three times daily over a period of eight days, the equivalent of taking 0.112 g of As_2O_3 .¹⁰

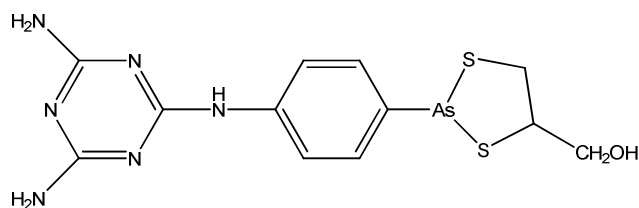


Figure 1.1 - Structure of Melarsaprol (Mel B), used to treat African sleeping sickness

Sleeping sickness is a disease that still runs rampant throughout Africa causing fever, headaches, and joint pains in the early stages, and then anaemia, heart and kidney disease, and if left untreated, irreversible neurological damage, and finally death.⁴ An arsenic based compound Melarsaprol, sold under the name Mel B (Figure 1.1), is still currently used as it is one of the cheapest cures. The alternative drug, Eflornithine doesn't contain arsenic, and is deemed to be much safer, however a typical dose costs US\$210 per course, compared to US\$50 for Melarsaprol.¹

The use of arsenicals in the medical field has been revived in more recent years with the discovery that arsenic trioxide (As_2O_3) shows signs of being able to cure acute promyelocytic leukemia (APL), a rare and fatal form of cancer that affects mostly young people, averaging two in every million.¹¹ Trials were started in the United States¹² in 1996 after learning of results published by Chinese researchers. They reported their success with this 'new' treatment on 16 patients that had not responded to other anticancer treatments.¹³ Solubilised As_2O_3 was administered intravenously at a rate of 10 mg day^{-1} for 45 days, at which time bone marrow remission was attained in two thirds of the patients.¹³

The rediscovery of As_2O_3 has led to many medical trials being undertaken. Many cancers such as liver, pancreatic, gastric, ovarian, cervical, prostate, renal, bladder, breast and lung cancer have had some form of trials with As_2O_3 , the results however are varied.¹⁴

Paradoxically, this once ancient treatment, given out as a magical cure for many ailments, is now sold as an expensive, 'pharmaceutically acceptable' (soluble) patented¹⁵ drug, going by the name Trisenox.¹⁶

1.1.1 Salvarsan

Salvarsan, also known as arsphenamine or simply 606, was the 606th compound to be tested for biological activity by Ehrlich's group against *Trepenoma pallidum*, the spirochete bacterium responsible for causing syphilis.⁴ Ehrlich was in search of a 'magic bullet', a one shot cure, and Salvarsan seemed to be just that for syphilis.¹ A more soluble derivate of Salvarsan, Neosalvarsan was the drug of choice to cure syphilis right up until the widespread use of penicillin.

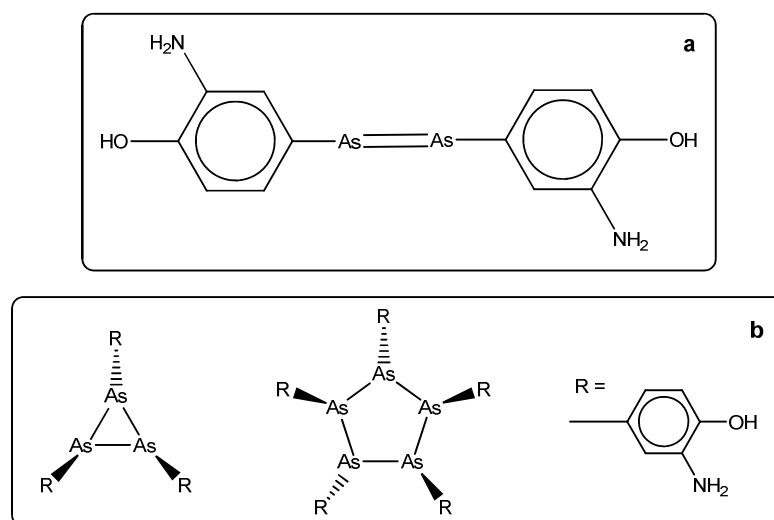


Figure 1.2 – (a) Ehrlich's proposed structure of Salvarsan, (b) main constituents of Salvarsan as published by Lloyd *et al.*¹⁷

Ehrlich had assigned Salvarsan a diarsene type structure, shown in Figure 1.2a, but recently the actual structure has been under scrutiny.^{18, 19} We now know that As=As double bonds are only formed when the substituents are bulky.²⁰ Steric crowding makes the formation of a ring unfavourable. The 3-H₂N-4-HOC₆H₃ substituent is not particularly bulky however, and so the formation of a cyclic structure is likely. Lloyd *et al.* reported the first definitive evidence that Salvarsan formed cyclic structures.¹⁷ The evidence was high resolution mass spectral data showing a series of ions assigned to cyclic structures of the form $[(RAs)_n + H]^+$ for $n = 3-8$.¹⁷ It appears that a solution of Salvarsan actually contains multiple $(RAs)_n$ compounds, predominantly $n = 3$ and 5 (Figure 1.2b).

1.1.2 The arsenic eaters of Styria

A group of people in an Styria, Austria, took to the idea of arsenic's medicinal properties a little more than most would have deemed beneficial. In the 1800's, rumours extended to the United Kingdom of a group of people that consumed potentially fatal doses of white arsenic (As_2O_3) or realgar (As_2S_2) every 2-3 days over periods of 30 or more years.¹ The usual amount of arsenic consumed was 300-400 mg each time, well above the medically acknowledged lethal dosage of 70-180 mg As_2O_3 .¹⁰ Although they appear to have rather deadly eating habits, they apparently lived long, healthy lives.

The men who ate the arsenic claimed it helped them to breathe easier while hiking at higher altitudes, as well as increasing their courage and sexual potency.¹⁰ The women took arsenic to improve their complexion by making their cheeks red, and make them plump, which was a favourable feminine trait at the time.¹⁰ The reddening of the cheeks was a result of arsenic damaging the delicate blood vessels near the surface of the skin.⁵ The group as a whole also commented on its ability to aid in the digestion of heavy meals, and ward off infectious diseases.¹⁰

The arsenic was typically eaten sprinkled over bread with bacon. The fat in the bacon apparently reduced the absorption of the arsenic. When someone first started taking arsenic, the dosage started at about 10 mg, and was slowly increased up to the maximum dosage of 300-400 mg over a period of weeks, at which the dosage was then sustained.¹

There was initially much doubt that a group of peasants from Styria could manage to find a safe dosage of arsenic that appeared to be effective, when leading practitioners around the world had been trying to do the same thing with little success.¹⁰ To dispel all doubt, two arsenic eaters were invited to a conference in Graz, Austria where one consumed 400 mg As_2O_3 and the other 300 mg orpiment (As_2S_2) in front of the audience.¹⁰ The urine was then analysed and clearly showed the presence of significant levels of arsenic.¹⁰

The downside of taking such large amounts of arsenic, is that it interferes with iodine in the body. Iodine is an important trace element required by the

thyroid, which is responsible for controlling many important metabolic processes.⁵ Goitre, caused by an iodine deficiency, was a prevalent disease amongst the arsenic eaters, and because of this it wasn't uncommon for children to have stunted physical and mental growth.⁵

1.2 The toxicity of arsenic

Even in light of all the medicinal benefits that arsenic has been shown to be capable of, the first thing that comes to mind of most when the word arsenic is said, is the idea of poison. The toxicity of arsenic is dependant on its form, primarily the oxidation state. Trivalent arsenicals are generally more toxic than their pentavalent counterparts.

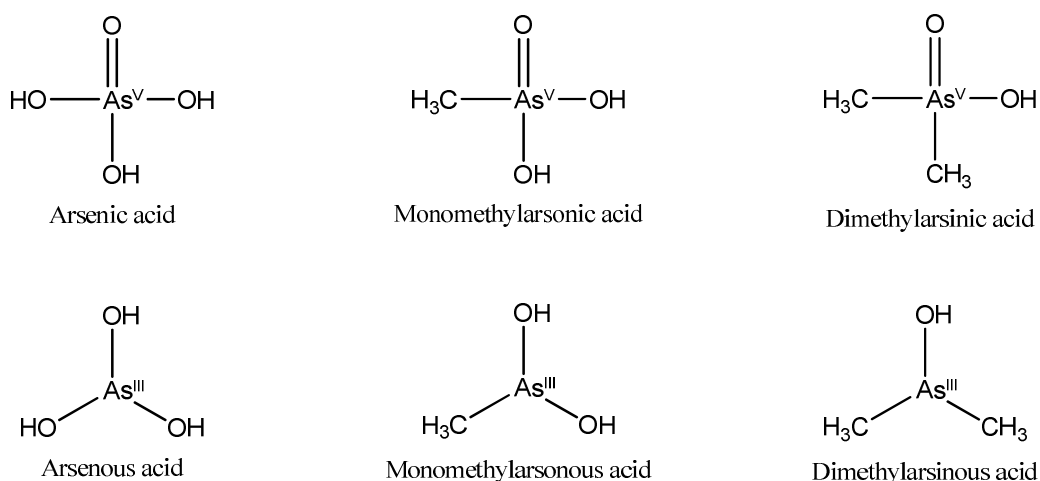


Figure 1.3 – Arsenic and arsenous acid and their methylated derivatives

The unpleasant nature of arsenic can wreak havoc on the human body. Acute poisoning can show symptoms such as abdominal pain, nausea, severe diarrhoea, and vomiting, or in more serious cases, damage to the peripheral nervous system and brain.²¹ The controlled treatment for acute arsenic poisoning is not clearly documented by today's medical standards, and effective chelation drugs are not always available in emergency departments.²² A report was published whereby two patients were successfully treated for arsenic overdoses by chelation therapy using dimercaptosuccinic acid (DMSA).²² DMSA is a more water-soluble derivative

of British Anti-Lewisite (dimercaprol), which was developed during World War II as an antidote to the arsenic chemical weapon Lewisite.¹

Chronic arsenic exposure via inhalation or ingestion have been studied extensively and clearly show the increased risk of respiratory cancer.²³ Other effects seen have been skin cancers, damage to the peripheral nervous system, anaemia, and damage to the blood vessels.²³

One of the widely known cases of acute mass arsenic exposure occurred in 1900 in England. Doctors saw a large increase in patients that showed peripheral neuritis (damage of the peripheral nervous system). The patients were typically working class beer drinkers, and so the symptoms were written off as results of alcoholism.¹ Questions started being asked when women and their breastfed children also suffered similar symptoms. There were approximately 6000 people affected by this new outbreak and at least 70 fatalities.²² The cause and source of the symptoms were traced back to the sugars used in the beer brewing process. The sulfuric acid used to convert cane sugar into the glucose/fructose mixture required for brewing contained up to 1.5% arsenic, which was then carried on into the brewing process, resulting in the contamination of the beer.¹ Needless to say, the suppliers of the brewing sugars had to discard their contaminated stock, totalling around 700 tons, forcing them into liquidation.¹

The exact mechanism of arsenic's toxicity is not known for sure but there are many hypotheses about possible actions. Firstly it is dependant upon which oxidation state the arsenic is in. The trivalent arsenic compounds, both inorganic and methylated, are thought to bind to thiol groups in proteins, inhibiting or completely halting their activity.²⁴ Pentavalent arsenic compounds are thought to replace phosphate in important biochemical processes because of their chemical similarities.²⁴ One of these processes is the conversion of ATP, to ADP a process that releases the energy stored in the cells, required the metabolism to function.²⁴ The arsenic analogues formed when replacing phosphorus are unstable, and hydrolysed in the body,

breaking down the conversion process, essentially starving the cells of energy.²⁴

1.3 Uses of arsenic

The use of arsenic based compounds are still common throughout the chicken breeding industry. The main compound used is 3-nitro-4-hydroxy phenyl arsonic acid, also called Roxarsone. It is used as a feed additive at about 50 ppm to prevent parasites in the intestinal tracts of chickens and promote growth.^{25, 26} An improvement in tissue pigmentation is also seen, which can be likened to the Victorian women who took arsenic trioxide to obtain a pale complexion.²⁵ Although Roxarsone has been shown to increase the weight of chickens by 4.1 %, the majority of the arsenic passes straight through the chickens and into the bedding material, typically corn husks and wood chips.¹ The bedding is usually disposed of by spreading it over fields, the arsenic present in the bedding however, eventually ends up in the soil creating the potential for harmful levels of arsenic if the same land is being used for prolonged periods of time.¹

Chromated copper arsenate (CCA) is the most common treatment to preserve timber and is applied using vacuum pressure impregnation.^{1, 27}

In the recent race to create high temperature superconductors, arsenic appears to be one of the elements of choice to obtain the required properties. High temperature superconductors are materials that exert no electrical resistance at temperatures higher than 30 K. A new generation of superconductors have been published one after the other slowly raising the bar. ($\text{LaO}_{1-x}\text{F}_x\text{FeAs}$) becomes a superconductor at 26 K, closely followed by ($\text{SmO}_{1-x}\text{F}_x\text{FeAs}$) at 43 K, and ($\text{PrO}_{1-x}\text{F}_x\text{FeAs}$) at 52 K.²⁸ The compounds are particularly unusual as they contain iron, which is magnetic, and previously magnetism and superconductivity were thought not to mix.²⁸

While historically well studied and interesting, there are still areas that can usefully be re-investigated using modern analytical techniques.

1.4 Preparations of arsonic acids and arseno compounds

The two major compounds discussed in this thesis are arsonoacetic acid, $\text{H}_2\text{O}_3\text{As}^{\text{V}}\text{CH}_2\text{COOH}$ and arsenoacetic acid, nominally $(\text{As}^{\text{I}}\text{CH}_2\text{COOH})_2$; the traditional preparations of these two classes of compounds are outlined below.

1.4.1 Arsonic acids

Arsonic acids are of the form $\text{H}_2\text{O}_3\text{AsR}$ and can be prepared in many ways; the three most common methods are described below.

The Bart reaction forms arsonic acids by reacting aromatic diazo compounds with sodium arsenite (Na_3AsO_3) under alkaline conditions.²⁹



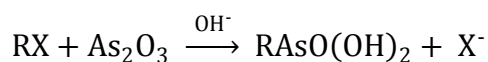
This reaction was patented in 1910.³⁰ Although the reaction must be carried out under alkaline conditions, the pH must be controlled as the reaction relies on the evolution of nitrogen, which does not occur at high pHs. Typically sodium carbonate is used as a buffer and can significantly increase yields.³¹

Aromatic amines, phenols, and phenyl ethers can be arsonated by the Béchamp reaction.²⁹



Ehrlich used this reaction early on in his organic arsenic research to study arsanilic acid. Amines undergoing the Béchamp reaction generally give poor yields (< 25%) however, the reaction is still useful as it works with both electron repelling and attracting substituents in the ring.²⁹

The most widely used preparation for alkylarsonic acids is the Meyer reaction.³² It follows the general scheme:



The reaction proceeds most rapidly with alkyl iodides, however bromides and chlorides are also used successfully.²⁹ Primary halides react readily, secondary halides only slowly, usually with some difficulty, and tertiary halides do not react at all.³³ The Meyer reaction has been adapted to work with aromatic halides, although not as readily; this is known as the Rosenmund reaction.³⁴

1.4.2 Arseno compounds

The exact structures of arseno compounds have been a topic of hot debate. Early on they were typically assigned diarsene (RAs=AsR) structures. There were also suggestions that the actual structures should have been polymeric³⁵ or cyclic³⁶.

The most common method for the synthesis of arseno compounds is by the reduction of arsonic acids (RAsO(OH)_2), arsenoso compounds ($(\text{RAsO})_x$), arsonous acids (RAs(OH)_2), or dihaloarsines (RAsX_2). The best reducing agents are either phosphorous acid or hypophosphorous acid.²⁹

Arseno compounds can also be obtained via the oxidation of primary aromatic arsines. The arsines however, are not air stable, and difficult to prepare, limiting the use of this method.²⁹

1.5 Usage and history of arsono- and arsenoacetic acid

1.5.1 Arsonoacetic acid

The first publication of arsonoacetic acid was by Palmer in 1923.³⁷

The disodium salt has been used to treat anaplasmosis (a parasitic disease), and as a stimulant in nervous diseases in cats.³⁸

Arsonoacetic acid has not featured much in human medicine, a Chinese patent however, was filed in 2003 for arsonoacetic acid and its methyl or ethyl derivatives as chemotherapeutic drugs against liver cancer.³⁹

1.5.2 Arsenoacetic acid

Arsenoacetic acid is synthesised by reducing arsonoacetic acid in an aqueous H_2SO_4 solution. The first synthesis was published in 1923 in the same publication as arsonoacetic acid.^{37, 40} A patent for the synthesis of many aliphatic arseno compounds, including arsenoacetic acid was issued in 1931.⁴¹

Although the aliphatic arseno compounds generally show lower biological activity than their aromatic counterparts, arsenoacetic acid has been used in many applications, both medical and otherwise, since its discovery. A patent was issued in 1970 detailing its use to treat timber as a fire retardant.⁴² In 2004, another patent for this very same compound was issued, this time not for treating timber, but rather treating premenstrual syndrome.⁴³ In the equine world, there appears to be an emerging problem of chronic fatigue syndrome, luckily arsenoacetic acid has been tested and shown to be an effective treatment.⁴⁴

The originally proposed structure of arsenoacetic acid is shown in Figure 1.4.

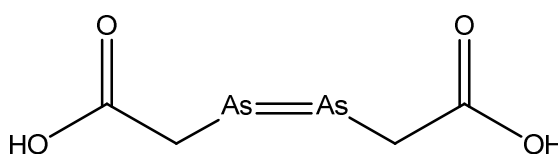


Figure 1.4 – Palmer's proposed structure of arsenoacetic acid

At the time, this structure would have satisfied all the functional group tests and elemental analyses, and even today in well-respected literature, such as the Merck Index,³⁸ this is how arsenoacetic acid is depicted. In light of the work done by Lloyd *et al.*¹⁷ on Salvarsan, it was likely that this compound formed cyclic arseno structures of the form $(\text{RAs})_n$, rather than the unfavourable $\text{As}=\text{As}$ bond. Using the arsenal of analytical techniques not available back in the 1920's such as mass spectrometry, NMR, and X-ray crystallography, the exact structure of arsenoacetic acid has been uncovered and will be discussed later on in this thesis.

1.6 X-ray crystallography

Crystal structures of cyclic arseno compounds of various sizes have been published showing 3⁴⁵, 4^{46, 47}, 5⁴⁸⁻⁵⁰ and 6⁵¹⁻⁵³ membered rings. The majority contain aromatic substituents as they have proven to be more medicinally significant, easier to synthesise, more stable and crystallise more readily. The first published cycloarsenic crystal structure was of arsenomethane, dating back to 1957.⁴⁸ The crystal structure of arsenomethane revealed a puckered arsenic ring in a chair conformation with As-As-As angles of approximately 90° and As-As bond lengths averaging 4.1 Å. All cycloarsenic structures to date have formed highly puckered rings in chair conformations with angles near 90°. The average bond lengths seen in higher quality crystal structures of 2.459 Å is much shorter to that measured in arsenomethane.⁵²

X-ray crystallography is one of the few definitive methods for determining the exact structure of these cycloarsenic structures, and has proven invaluable in this study.

2. Experimental

2.1 General

All water was deionised, and commercial drum grade organic solvents were used without further purification, unless otherwise noted.

2.2 Instrumental techniques

2.2.1 EDX spectroscopy

EDX spectroscopy was carried out on a Hitachi S-4700 field energizing scanning electron microscope (SEM), conducted at 20 kV with a 30° takeoff angle.

2.2.2 FT-IR spectroscopy

All samples were dried overnight *in vacuo* over silica before being run as KBr disks on a PerkinElmer Spectrum 100 FT-IR spectrometer. Data was processed using the PerkinElmer Spectrum software.

2.2.3 GC-MS

Samples were run on a HP6890 Series GC system with a non-polar ZB-5 column (30 m × 0.25 mm, 5% phenyl 95% dimethylpolysiloxane, 25 µm film thickness) connected to a HP 5973 Mass Selective Detector (TIC, mass scanned: 42 – 650 *m/z*) using an ESI ionisation source.

1 µL was injected onto the column at 60 °C, held for 0.5 min, increased to 150 °C at 30 °C min⁻¹, and then up to 285 °C at 10 °C min⁻¹ where the temperature was held for 15 min. Helium carrier gas flow rate was 2 mL min⁻¹, 20 psi.

2.2.4 High-resolution mass spectrometry

All spectra were obtained on a Bruker MicrOTOF mass spectrometer, with an ESI source and TOF detector using default settings in negative ion mode. The

mass spectrometer was calibrated prior to each use with a sodium formate solution.

2.2.5 HPLC

Samples were loaded *via* a Rheodyne 7725i injector with a 2 mL loop and eluted at 1 mL min⁻¹ through a Hamilton PRP-X100 anion exchange column. A 5:95 acetonitrile:water eluent (degassed prior to used by sonication), containing either 50 mmol sodium hydroxide, 40 or 100 mmol pyridine, was run isocratically by a Waters 515 HPLC pump. UV detection was by a Waters 996 PDA detector (190 – 400 nm) and data processed using Empower Pro software.

2.2.6 NMR spectroscopy

¹H and ¹³C{¹H} NMR experiments were run on a 300 or 400 MHz Bruker Avance series machine at ambient temperature (303 K). Samples were run in 5 mm tubes and, unless otherwise noted, used D₂O as the lock solvent. ¹H spectra were calibrated to the HOD peak occurring at 4.79 ppm,⁵⁴ ¹³C spectra were left unchanged as there were no solvent peaks.

When run in pyridine-d₅, ¹H spectra were calibrated to the most downfield solvent peak at 8.74 ppm, and ¹³C to 150.3 ppm.

Where required, resolution enhancement was used by applying line broadening (LB) and Gaussian broadening (GB) parameters of -2.5 and 0.33 respectively. Linear prediction was also used. Spectra were then processed using these values.

2.3 Synthesis of barium arsonoacetic acid – (BaO₃AsCH₂COO)₂Ba

Barium arsonoacetic acid was prepared based on the synthesis by Palmer.⁴⁰ Arsenic trioxide (10 g, 51 mmol) was added to a hot alkaline solution (10 g NaOH, 0.4 mol, 30 mL H₂O) and cooled to room temperature. Chloroacetic

acid (4.8 g, 51 mmol) was added and stirred for one hour. The clear solution was acidified with glacial acetic acid (16 mL) and after cooling to 40 °C, the precipitated excess arsenic trioxide was filtered off by suction and washed with water. The filtrate was poured into a hot barium chloride solution (18.5 g BaCl₂·2H₂O, 76 mmol, 60 mL H₂O) and stirred for five minutes. Barium arsonoacetic acid was filtered by suction after the solution was allowed to stand overnight, and washed thoroughly with water (30 g, 75%).

IR: $\nu(\text{C=O})$ 1635 (s) cm⁻¹

EDX: 3:2 Ba:As (molar ratio)

2.4 Synthesis of sodium arsonoacetic acid – Na₂O₃AsCH₂COONa·H₂O

Barium arsonoacetic acid (22 g, 28 mmol) was added to a hot solution of anhydrous sodium sulfate (10.7 g, 75 mmol, 50 mL H₂O) and stirred for one hour at room temperature. Barium sulfate was filtered and the filtrate concentrated using a rotary evaporator and recrystallised from water as the monohydrate (12.95 g, 85%).

¹H NMR: [D₂O] δ 3.16 (s, CH₂) ppm

¹³C{¹H} NMR: [D₂O] δ 42.6 (s, CH₂), 172.6 (s, COO⁻) ppm

IR: $\nu(\text{C=O})$ 1620 (s) cm⁻¹

HRMS: [H₂O] See Table 2.1

Table 2.1 - HRMS data for sodium arsonoacetic acid, where R = CH₂COO⁻

Ion	Intensity (%)	Measured <i>m/z</i>	Calculated <i>m/z</i>	$\Delta m/z$
[(H ₂ O ₃ AsR) ₂ +Na] ⁻	2.7	388.853	388.845	0.008
[(H ₂ O ₃ AsR) ₂ +H] ⁻	3.6	363.868	366.863	0.005
unknown	7.8	313.267		
[C ₂ As ₂ H ₇ O ₅] ⁻	12.8	260.878	260.873	0.005
[HNaO ₃ AsR] ⁻	7.3	204.915	204.909	0.006
[H ₂ O ₃ AsR] ⁻	34.4	182.932	182.927	0.005
unknown	6.9	157.127		
[H ₂ O ₃ AsCH ₂] ⁻	100	138.943	138.938	0.005
unknown	8.6	123.919		
unknown	13.8	120.932		

2.5 Synthesis of arsonoacetic acid – H₂O₃AsCH₂COOH

As described by Palmer³⁷; barium arsonoacetic acid (5.4 g, 7 mmol) was stirred in H₂SO₄ solution (1.2 mL H₂SO₄, 24 mL H₂O) for five hours and precipitated barium sulfate was filtered by suction. Solvent was removed *in vacuo* over conc. H₂SO₄ until crystallisation commenced. The free acid was extracted into absolute ethanol (6 mL) and remaining inorganic material filtered. Petroleum spirits (6 mL) was added, and dried over concentrated H₂SO₄ *in vacuo* until crystallisation commenced. Although a little unusual, the method was followed as written. The final product was washed with petroleum spirits (1.54 g, 60%).

Higher yields of much higher purity were obtained following a method described by Rozovskaya *et al.*⁵⁵ and Sparkes & Dixon⁵⁶. Barium arsonoacetic acid (1.3 g, 5.04 mmol) was stirred for 30 minutes with a sulfonated polystyrene resin (Amberlite® IR-120, 10 mL wet volume) in its H⁺ form, which can then be regenerated by stirring with 5% HCl. The solution was filtered and water removed using a rotary evaporator leaving a white powder, pure by microanalysis (0.50 g, 80%).

Found: C, 13.27; H, 2.78%; H₂O₃AsCH₂COOH requires: C, 13.06; H, 2.74%

^1H NMR: $[\text{D}_2\text{O}]$ δ 3.73 (s, CH_2) ppm

$^{13}\text{C}\{^1\text{H}\}$ NMR: $[\text{D}_2\text{O}]$ δ 39.3 (s, CH_2), 168.0 (s, COO^-) ppm

IR: $\nu(\text{C}=\text{O})$ 1683 (s) cm^{-1}

HRMS: $[\text{H}_2\text{O}]$ See Table 2.2

Table 2.2 - HRMS data for arsonoacetic acid – $\text{H}_2\text{O}_3\text{AsCH}_2\text{COOH}$

Ion	Intensity (%)	Measured m/z	Calculated m/z	$\Delta m/z$
$[\text{3M-H}]^-$	15.6	550.804	550.798	0.006
$[\text{3M-H}_2\text{O-H}]^-$	16.4	532.793	532.787	0.006
$[\text{2M-H}]^-$	52.4	366.867	366.863	0.004
$[\text{2M-H}_2\text{O-H}]^-$	28.8	348.856	348.852	0.004
$[\text{C}_2\text{As}_2\text{H}_7\text{O}_5]^-$	8.5	260.875	260.873	0.002
$[\text{M-H}]^-$	100	182.929	182.927	0.002
$[\text{M-COOH}]^-$	30.3	138.940	138.938	0.002

2.6 X-ray crystal structure of arsonoacetic acid – $\text{H}_2\text{O}_3\text{AsCH}_2\text{COOH}$

Colourless block crystals of X-ray quality were grown by slow evaporation of a saturated aqueous solution of arsonoacetic acid at room temperature.

Data collection: Unit cell and intensity data were collected at the University of Canterbury on a Bruker Apex-II CCD Diffractometer, operating at 93 K. Absorption corrections were applied using semi-empirical methods (SADABS).⁵⁷

Solution and Refinement: All non-hydrogen atoms were found by direct methods option and subsequent difference maps. Hydrogen atoms were placed in calculated positions with the hydroxyl torsion angles calculated from electron density. All non-hydrogen atoms were refined anisotropically. Calculations were performed with SHELX97⁵⁸ programs and CIF validation was carried out using Platon.⁵⁹

Collection data: Crystal size: $0.40 \times 0.56 \times 0.60$ mm, temperature: 93 K, total reflections: 13348, unique reflections: 1764 (R_{int} 0.0548), range: $3.27^\circ < \theta < 32.61^\circ$, semi-empirical absorption correction $T_{\text{max,min}}$: 0.7464, 0.3155.

Crystal data: C₂H₅O₅As, M_r 183.98, orthorhombic, space group P2₁2₁2₁, a = 6.0904(3), b = 7.7557(4), c = 10.4713(5) Å, volume = 494.62(4) Å³, D_{calc} = 2.47 g cm⁻³, Z = 4, F(000) 360, μ(Mo-Kα) = 6.80 mm⁻¹.

Refinement details: Refinement on F² gave R₁ 0.0190 [I > 2σ(I)], wR₂ 0.0507 (all data), goodness-of-fit 1.188.

2.7 Synthesis of arsenoacetic acid – As_x(CH₂COOH)_x

Arsenoacetic acid was prepared based on the synthesis by Palmer.⁴⁰ Sodium arsonoacetic acid (12.5 g, 50 mmol) was added to a cold solution of conc. H₂SO₄ (22.5 mL), H₃PO₂ (47.6 mL, 50% in H₂O), H₂O (100 mL) and allowed to stand at room temperature under N₂ for three days. The orange precipitate was filtered, washed with water, and dried *in vacuo* over conc. H₂SO₄. The filtrate was allowed to stand under N₂ for another two days, and a second crop was obtained. Combined fractions (4.70 g, 70%).

Found: C, 17.40; H, 2.26%; As_x(CH₂COOH)_x requires: C, 17.93; H, 2.26%

¹H NMR: [Pyridine-*d*₅] δ 3.59 (s, CH₂) ppm

¹³C{¹H} NMR: [Pyridine-*d*₅] δ 26.9 (s, CH₂), 174.1 (s, COOH) ppm

IR: ν(C=O) 1681 (s) cm⁻¹

HRMS: [1:1 CH₃CN:H₂O] (with the addition of pyridine) See Table 2.3

Table 2.3 - HRMS data for arsenoacetic acid – As_xR_x, where R = CH₂COOH

Ion	Intensity	Measured <i>m/z</i>	Calculated <i>m/z</i>	Δ <i>m/z</i>
[(AsR) ₁₁ -H] ⁻	0.8	1472.275	1472.276	0.001
[(AsR) ₁₀ -H] ⁻	0.6	1338.342	1338.341	0.001
[(AsR) ₉ -H] ⁻	1	1204.409	1204.406	0.003
[(AsR) ₈ -H] ⁻	0.2	1070.473	1070.471	0.002
[(AsR) ₇ +O-H] ⁻	4.4	952.528	952.531	0.003
[(As ₇ R ₆ -2H] ⁻	0.2	876.517	876.515	0.002
[(AsR) ₆ -H] ⁻	100	802.602	802.602	0.000
[(As ₆ R ₅ -2H] ⁻	1.4	742.581	742.58	0.001
[(AsR) ₅ -H] ⁻	50.2	668.667	668.667	0.000

$[(As_5R_4-2H)^-]$	7.8	608.646	608.646	0.000
$[(AsR)_4-H]^-$	12.6	534.732	534.732	0.000
$[As_4R_3-2H]^-$	5.4	474.711	474.711	0.000
$[(AsR)_3-H]^-$	11.5	400.798	400.797	0.001

2.8 X-ray crystal structure of cyclohexaarsenoacetic acid – $As_6(CH_2COOH)_6 \cdot 6C_5NH_5$

Colourless block crystals of X-ray quality were grown by cooling a saturated pyridine solution of arsenoacetic acid from room temperature to 4 °C.

Data collection: Unit cell and intensity data were collected at the University of Auckland on a Bruker Apex-II CCD Diffractometer, operating at 90 K. Absorption corrections were applied using semi-empirical methods (SADABS).⁵⁷

Solution and Refinement: The three unique As atoms were found by the Patterson methods option of SHELX97,⁵⁸ all other non-hydrogen atoms were found in subsequent difference maps. Methylene hydrogen atoms were placed in calculated positions, while the OH hydrogen atoms were located in a difference map and then refined. All non-hydrogen atoms were refined anisotropically. CIF validation was carried out using Platon.⁵⁹

Collection data: Crystal size: 0.29 × 0.20 × 0.17 mm, temperature: 90 K, total reflections: 37809, unique reflections: 6128 (R_{int} 0.0384), range: 1.82° < θ < 28.10°, semi-empirical absorption correction $T_{max,min}$: 0.5504, 0.3908.

Crystal data: $C_{42}As_6H_{48}O_{12}N_6$, M_r 1278.38, triclinic, space group $P\bar{1}$, $a = 10.1456(1)$, $b = 11.6233(1)$, $c = 12.4298(2)$ Å, $\alpha = 113.948(1)$, $\beta = 92.378(1)$, $\gamma = 106.716(1)^\circ$, volume = 1261.85(3) Å³, $D_{calc} = 1.682$ g cm⁻³, $Z = 1$, $F(000)$ 636, $\mu(Mo-K\alpha) = 7.1073$ mm⁻¹.

Refinement details: Refinement on F^2 gave R_1 0.0221 [$I > 2\sigma(I)$], wR_2 0.0466 (all data), goodness-of-fit 1.035.

2.9 Synthesis of sodium arsenoacetic acid – $\text{As}_x(\text{CH}_2\text{COONa})_x$

The water soluble sodium salt of arsenoacetic acid was prepared as described by Palmer.³⁷ Arsenoacetic acid (0.50 g, 1.87 mmol) was added to an aqueous 5% sodium hydroxide solution (4 mL) and filtered. Ethanol (95%, 11 mL) was added to the filtrate and a yellow oil separated out. Upon standing at room temperature for several hours fine yellow-brown needles crystallised, washed with 95% ethanol and dried *in vacuo* over concentrated H_2SO_4 (0.44 g, 75%).

^1H NMR: [D_2O] δ 2.96 (s, CH_2) ppm

$^{13}\text{C}\{^1\text{H}\}$ NMR: [D_2O] δ 31.5 (s, CH_2), 180.2 (s, COO^-) ppm

HRMS: [1:1 $\text{CH}_3\text{CN}:\text{H}_2\text{O}$] (with the addition of pyridine) See Table 2.4

Table 2.4 - Selected HRMS data for sodium arsenoacetic acid, where $\text{R} = \text{CH}_2\text{COOH}$

Ion	Intensity (%)	Measured m/z	Calculated m/z	$\Delta m/z$
$[(\text{AsR})_6+3\text{Na}^+-4\text{H}^+]^-$	7.9	868.561	868.547	0.014
$[(\text{AsR})_6+2\text{Na}^+-3\text{H}^+]^-$	11	846.578	846.565	0.013
$[(\text{AsR})_6+\text{Na}^+-2\text{H}^+]^-$	7.6	824.598	824.584	0.014
$[(\text{AsR})_6-\text{H}^+]^-$	7.2	802.612	802.602	0.010
$[(\text{AsR})_5+3\text{Na}^+-4\text{H}^+]^-$	7.4	734.626	734.612	0.014
$[(\text{AsR})_5+2\text{Na}^+-3\text{H}^+]^-$	12.7	712.642	712.631	0.011
$[(\text{AsR})_5+\text{Na}^+-2\text{H}^+]^-$	31.7	690.661	690.649	0.012
$[(\text{AsR})_5-\text{H}^+]^-$	65.4	668.679	668.667	0.012
$[(\text{AsR})_4+3\text{Na}^+-4\text{H}^+]^-$	8.6	600.690	600.678	0.012
$[(\text{AsR})_4+2\text{Na}^+-3\text{H}^+]^-$	24.9	578.707	578.696	0.011
$[(\text{AsR})_4+\text{Na}^+-2\text{H}^+]^-$	36.5	556.724	556.714	0.010
$[(\text{AsR})_4-\text{H}^+]^-$	47.9	534.743	534.732	0.011
$[(\text{AsR})_3+2\text{Na}^+-3\text{H}^+]^-$	24.2	444.768	444.761	0.007
$[(\text{AsR})_3+\text{Na}^+-2\text{H}^+]^-$	100	422.788	422.779	0.009
$[(\text{AsR})_3-\text{H}^+]^-$	63.5	400.806	400.797	0.009

2.10 Attempted esterification of arsenoacetic acid – $(\text{AsCH}_2\text{COOCH}_3)_x$

Arsenoacetic acid (150 mg, 0.5 mmol) was stirred in SOCl_2 (20 mL, excess) with a catalytic amount of pyridine under N_2 as described by McMurry,⁶⁰ a clear red-orange solution resulted. The reaction was stirred until evolution of SO_2 and HCl gas stopped. The remaining SOCl_2 was removed by vacuum, and super-dry methanol (20 mL) was added while vessel was still under N_2 , forming a clear yellow solution. (Discussed in 3.2.7)

2.11 X-ray crystal structure of S_8

Yellow block crystals of X-ray quality were grown by slow evaporation of a crude methanol solution, from the attempted esterification of arsenoacetic acid, at room temperature.

Data collection: Unit cell and intensity data were collected at the University of Auckland on a Bruker Apex-II CCD Diffractometer, operating at 90 K. Absorption corrections were applied using semi-empirical methods (SADABS).⁵⁷

Solution and Refinement: All atoms were found by the direct methods of SHELX97⁵⁸ and refined anisotropically using subsequent difference maps. CIF validation was carried out using Platon.⁵⁹

Collection data: Crystal size: $0.27 \times 0.30 \times 0.30$ mm, temperature: 90 K, total reflections: 15373, unique reflections: 5429 (R_{int} 0.0196), range: $1.89^\circ < \theta < 27.86^\circ$, semi-empirical absorption correction $T_{\text{max,min}}$: 0.6039, 0.5745.

Crystal data: S_8 , M_r 256.48, monoclinic, space group $P2_1$, $a = 10.6736(1)$, $b = 10.7014(1)$, $c = 10.8139(1)$ Å, $\beta = 95.711(1)^\circ$, volume = $1229.06(2)$ Å³, $D_{\text{calc}} = 2.079$ g cm⁻³, $Z = 6$, $F(000)$ 768, $\mu(\text{Mo-K}\alpha) = 7.1073$ mm⁻¹.

Refinement details: Refinement on F^2 gave R_1 0.0208 [$I > 2\sigma(I)$], wR_2 0.0514 (all data), goodness-of-fit 1.090.

3. Results and Discussion

3.1 Arsonoacetic acid and its salts

3.1.1 Synthesis

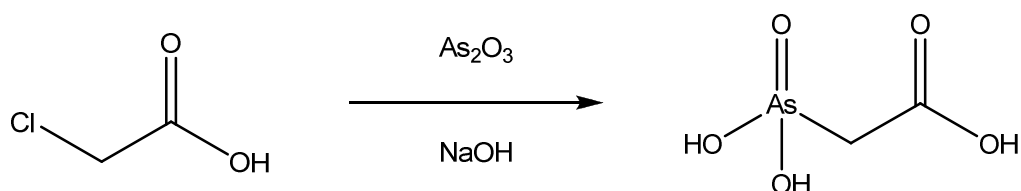


Figure 3.1 – Reaction scheme for arsonoacetic acid

Arsonoacetic acid was synthesised as a precursor to arsenoacetic acid. An excess of the relatively insoluble As_2O_3 was dissolved in a strong caustic solution. Palmer discovered the need for the excess by means of an iodometric study of the reaction, whereby a 0.1 M iodine solution was titrated to determine the concentration of arsenious acid, in the form Na_3AsO_3 .⁴⁰ Chloroacetic acid was then stirred with this solution, forming arsonoacetic acid. The excess As_2O_3 was later removed by acidifying the solution with glacial acetic acid, and filtering.

Stirring the crude filtrate with barium chloride formed a white precipitate, practically insoluble in water, making it easy to isolate by filtration alone. The barium salt could then be converted to the free acid. Palmer reported a method, as described in section 2.5, with an unusual workup. Once the free acid had been formed, by stirring with H_2SO_4 , and any excess solvent removed by vacuum, the free acid was then extracted into absolute ethanol, leaving behind other impurities. Petroleum spirits was then added, and removed immediately under vacuum. The reason for the addition of petroleum spirits is unknown, however while removing the solvent *in vacuo*, crystals of arsonoacetic acid do form, albeit in lower yields and purity than an alternative method reported by Rozoveskaya *et al.*⁵⁵

Rozovskaya *et al.* were using arsonoacetic acid for biological work and could not subject their enzymes to strong acids. By using a sulfonated resin to convert the arsonoacetic acid salt to the free acid, they avoided the use of any acids. Simply stirring the easily isolated barium salt with the resin, in water for 30 minutes, exchanged Ba^{2+} for H^+ resulting in high yields of the free acid, free from impurities. The reaction proceeded very rapidly despite the very poor solubility of barium arsonoacetic acid.

3.1.2 EDX analysis of barium arsonoacetic acid

Characterisation of the synthesised barium arsonoacetic acid was difficult as it is essentially insoluble in all solvents. This was intentional as it could then be easily separated from other by products in solution. Heavy metal analysis by EDX showed the molar ratio of barium to arsenic, 3:2 agreeing with the calculated value for $(\text{BaO}_3\text{AsCH}_2\text{COO})_2\text{Ba}$.

3.1.3 Discussion of X-ray crystal structure of arsonoacetic acid

The structure of arsonoacetic acid was determined by X-ray crystallography, shown below in Figure 3.2. It crystallises in the $P2_12_12_1$ space group and is isomorphous with the phosphorus analogue, phosphonoacetic acid ($\text{H}_2\text{O}_3\text{PCH}_2\text{COOH}$), providing a useful comparison.⁶¹

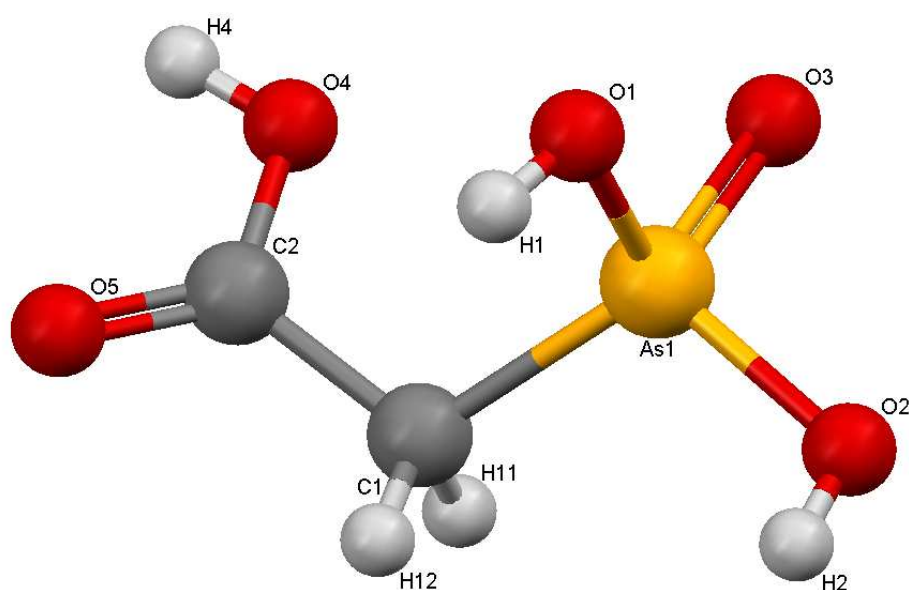


Figure 3.2 - The structure and labelling scheme of arsonoacetic acid

Table 3.1 - Selected bond lengths (Å) comparing arsono- and phosphonoacetic acid

Arsonoacetic acid		Phosphonoacetic acid		Δ
As1-O1	1.7013(13)	P-O1	1.544(2)	0.157
As1-O2	1.6461(12)	P-O2	1.494(2)	0.152
As1-O3	1.7072(13)	P-O3	1.544(2)	0.163
As1-C1	1.9185(17)	P-C1	1.799(2)	0.120
C1-C2	1.509(2)	C1-C2	1.503(2)	0.006
C2-O4	1.312(2)	C2-O4	1.305(2)	0.007
C2-O5	1.210(2)	C2-O5	1.216(2)	0.006

Four individual molecules occupy the unit cell, with significant intermolecular hydrogen bond interactions. The arsenic is distorted tetrahedral, with an average O-As-O angle of 107°, and O-As-C angle of 112°, deviating from the perfect tetrahedral angle of 109°. With respect to the carboxylic C2, the protonated O2 is *trans*, O1 and the unprotonated O3 are *gauche*. The dihedral angle between the carboxyl group and a plane through O2-As1-C1 is 43°.

The As-O and As-C bonds are longer than P-O and P-C bonds in phosphonoacetic acid partly because of the increased size of the arsenic atom, 1.07 and 1.19 Å for phosphorus and arsenic covalent radii respectively. Accounting for the difference in atom size, the As-O bonds are slightly weaker (longer) than the equivalent P-O bonds, possibly due to the slight increase in the electronegativity of phosphorus.

Using Mogul to compare bond lengths, angles, and torsion angles of similar systems in the Cambridge Crystal Database⁶² resulted in bond lengths and angles very close to the average values. The O3-As1-C1 bond angle of 117.4° however was the highest of seven similar compounds, the next highest being 115.1° and the O3-As1-O2 angle of 104.9° being one of the lower values of a set of 54 compared compounds.

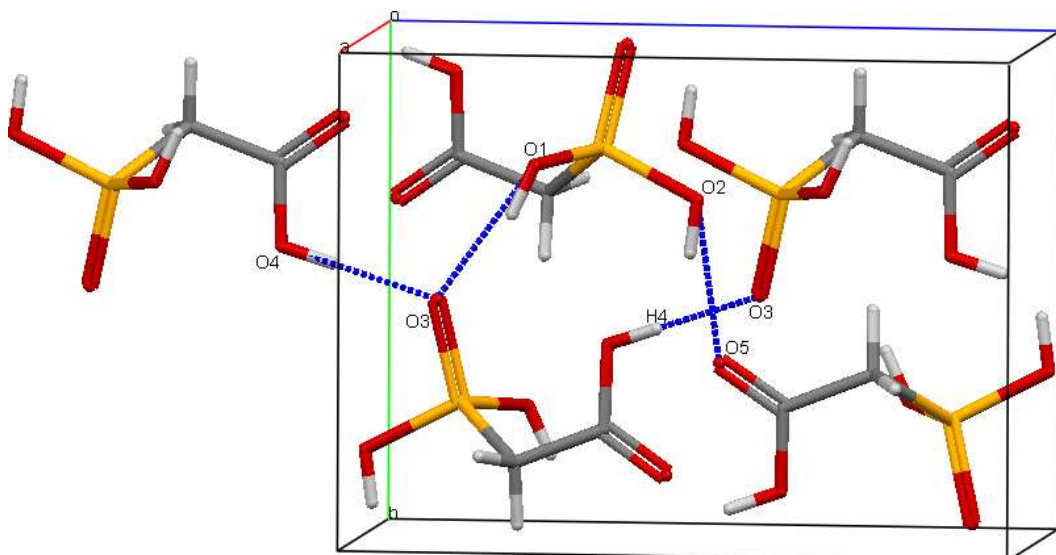


Figure 3.3 – Crystal packing diagram of arsonoacetic acid showing intermolecular hydrogen bonding

Table 3.2 - Hydrogen bonds for arsonoacetic acid (Å and °), hydrogen atoms were placed in calculated positions with refined hydroxyl torsion angles

D-H \cdots A	d(D-H)	d(H \cdots A)	d(D \cdots A)	\angle (DHA)
O2-H2 \cdots O5 ⁱ	0.84	1.82	2.612(2)	156.1
O1-H1 \cdots O3 ⁱⁱ	0.84	1.79	2.605(2)	162.8
O4-H4 \cdots O3 ⁱⁱⁱ	0.84	1.71	2.544(2)	170.6

Symmetry transformations used to generate equivalent atoms:

(i): $-x+3/2, -y, z-1/2$; (ii): $-x+2, y-1/2, -z+3/2$; (iii): $-x+3/2, -y+1, z+1/2$

All oxygen atoms are involved in intermolecular hydrogen bonding, as either a donor or acceptor, none as both, or intramolecularly. The unprotonated arsonic oxygen, O3 accepts two H atoms from O1 and O4. The carboxyl oxygen O5 accepts a H atom from O2, shown above in Figure 3.3. This is an identical hydrogen bonding system to phosphonoacetic acid, and appears preferable to the typical carboxyl dimer often seen.

The short distances between the donor and acceptor oxygen atoms indicate strong hydrogen bonding interactions. Brown suggests that a bond in the region of 2.4–2.7 Å is a strong hydrogen bond.⁶³ There is also a correlation between the D \cdots A and the D-H \cdots A angle, the stronger the hydrogen bond, the

closer the angle is to 180° .⁶⁴ This can be clearly seen with $O4-H4\cdots O3$, the shortest $D\cdots A$ distance, having an angle of 170° , whereas $O2-H2\cdots O5$ and $O1-H1\cdots O3$, being slightly longer and therefore weaker, have an angle closer to 160° .

3.1.4 Discussion of FT-IR results

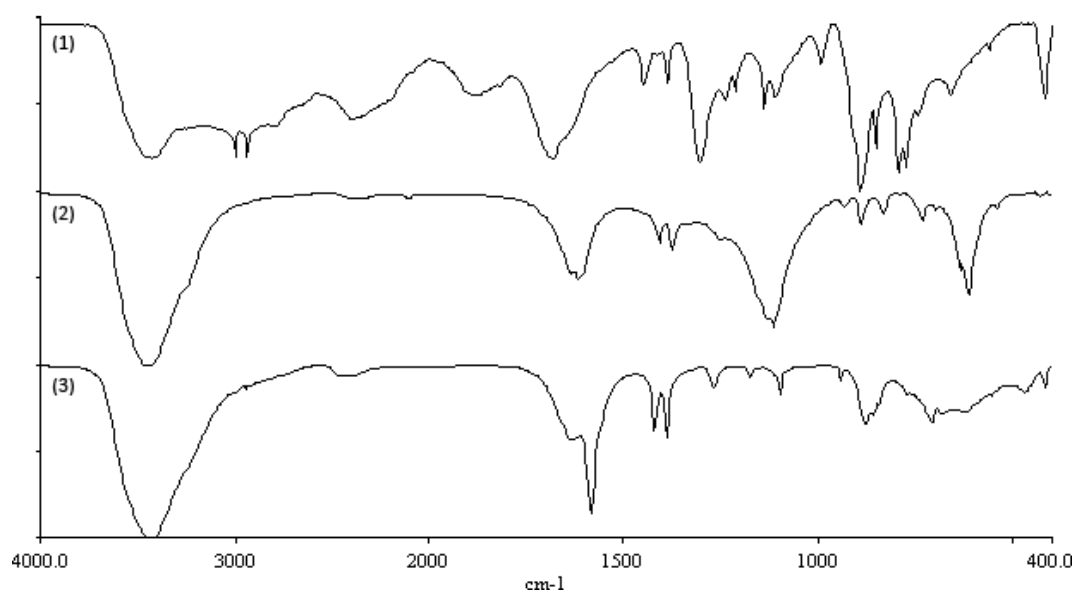


Figure 3.4 - FT-IR spectra of (1) arsonoacetic acid, (2) sodium arsonoacetic acid, (3) barium arsonoacetic acid, KBr disc

Arsonoacetic acid and its salts exhibit the typical carboxylic acid peaks as outlined by Colthup *et al.*⁶⁵ Some features in the functional group region ($4000 - 1000\text{ cm}^{-1}$) are exhibited in all three compounds, the major peaks are summarised in Table 3.3.

Table 3.3 - Summary and comparison of FT-IR data for the barium salt, sodium salt and free acid of arsonoacetic acid (cm⁻¹)

	Free acid (2)	Na salt (3)	Ba salt (4)
OH stretch (broad)	3420 (s)	3430 (vs)	3420 (vs)
Overtone + combination	2550-2300 (w)	2550-2300 (w)	2550-2300 (w)
C=O stretch	1683 (s)	1620 (s)	1635 (s)
CH ₂ bending and scissoring	1448 (m)	1408 (m)	1422 (m)
	1388 (m)	1376 (m)	1390 (m)
As=O	892 (s)	891 (w)	881 (m)

(w) = weak, (m) = medium, (s) = strong, (vs) = very strong

A very strong, broad OH stretch peak can be seen for both the barium and sodium salts, these both crystallise as hydrates, whereas the free acid is anhydrous. This peak in the free acid is from the carboxyl and arsonic hydroxyl groups. Two sharp peaks are clearly visible in the free acid at 3000 and 2936 cm⁻¹, from CH₂ symmetric and asymmetric stretching. Upon closer inspection, these peaks are also visible for the salts, however the broader OH peak overpowers them. The weak shoulder at 2550 – 2300 cm⁻¹ may be caused by overtones, and combinations of C-O stretches and OH deformation vibrations;⁶⁶ Braunscholtz *et al.* however suggest this peak should be assigned to OH stretching under strong hydrogen bonding conditions.⁶⁷ From this it could be reasoned that the free acid has a much more intense peak because of the strong intermolecular hydrogen bonding network. It is likely that not all hydroxyl groups have been exchanged during the synthesis of the salts and so still exhibit a weaker OH peak. The water from the hydrate could also contribute to this region. The broad peak at 1116 cm⁻¹ in sodium arsonoacetic acid appears to be from residual sulfate. Bardos *et al.* suggest the peak at 880 – 900 cm⁻¹ is from As=O stretching.⁶⁸

3.1.5 Discussion of HRMS results

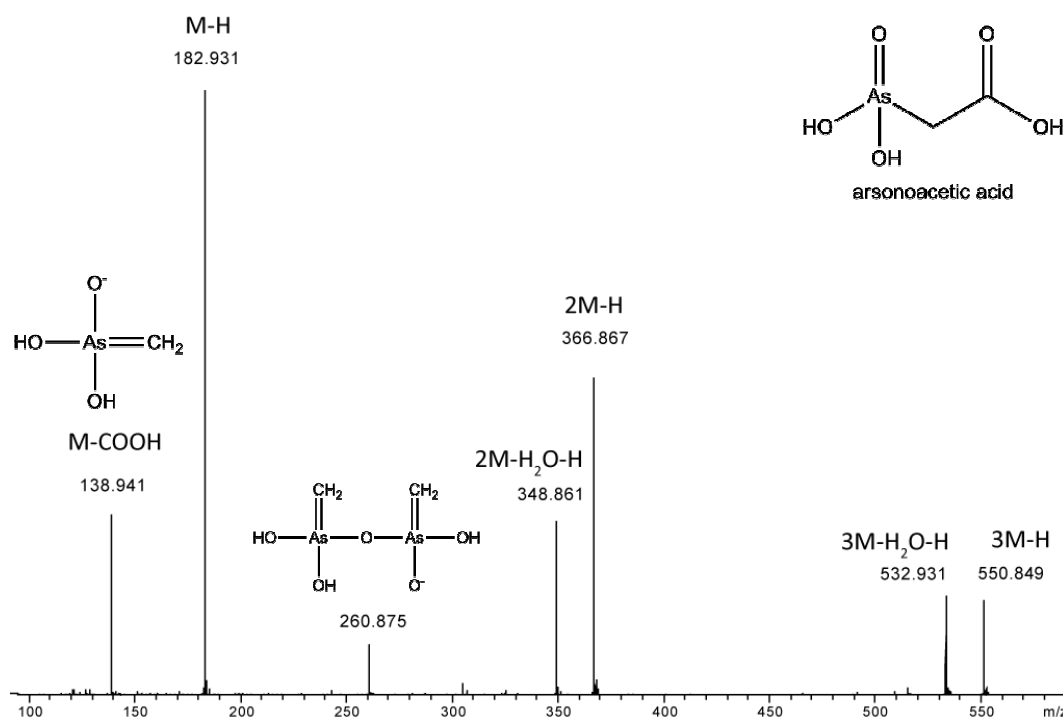


Figure 3.5 - HRMS of arsonoacetic acid in H₂O, negative ion mode

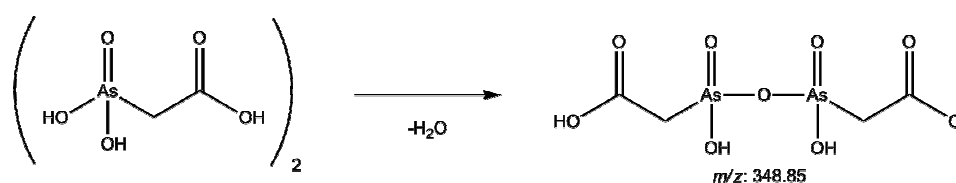


Figure 3.6 - Scheme for the formation of the peak at m/z 348.86 in the HRMS spectrum of arsonoacetic acid (Figure 3.5)

The free acid in H₂O has a very clean spectrum with readily assignable peaks. The series of [M-H]⁻, [2M-H]⁻ and [3M-H]⁻ are the three most abundant peaks, with the 2M and 3M also showing peaks 18.011 Da lower. This is from the condensation of two molecules with a loss of H₂O, shown in Figure 3.6. The loss of the carboxyl group can also be seen, 44 Da lower than [M-H]⁻ giving [H₂O₃As=CH₂]⁻ (m/z 138.941). This rearrangement ion is comparable to that of an ylide, explaining its stability.

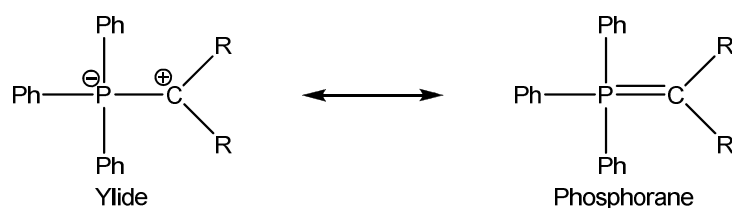


Figure 3.7- Structure of a phosphonium ylide and its resonance phosphorane form

Ylides are stable, neutral molecules that contain an adjacent negative and positive charge but are commonly represented by resonance structures (Figure 3.7).⁶⁹ Ylides are commonly seen in organic syntheses as reagents or reactive intermediates, the Wittig reaction being one of the more common reactions.

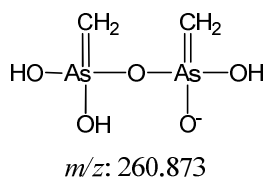


Figure 3.8 - Proposed structure of 260.877 Da ion in arsonoacetic acid mass spectrum

The smallest peak is at 260.877 Da, and is assignable to $[C_2As_2H_7O_5]^-$ with an *m/z* of 260.873. A plausible structure is shown in Figure 3.8 which could come about from the condensation reaction of two ylide type rearrangement ions.

The mass spectrum of the sodium salt was obtained in H₂O and is shown in Figure 3.9.

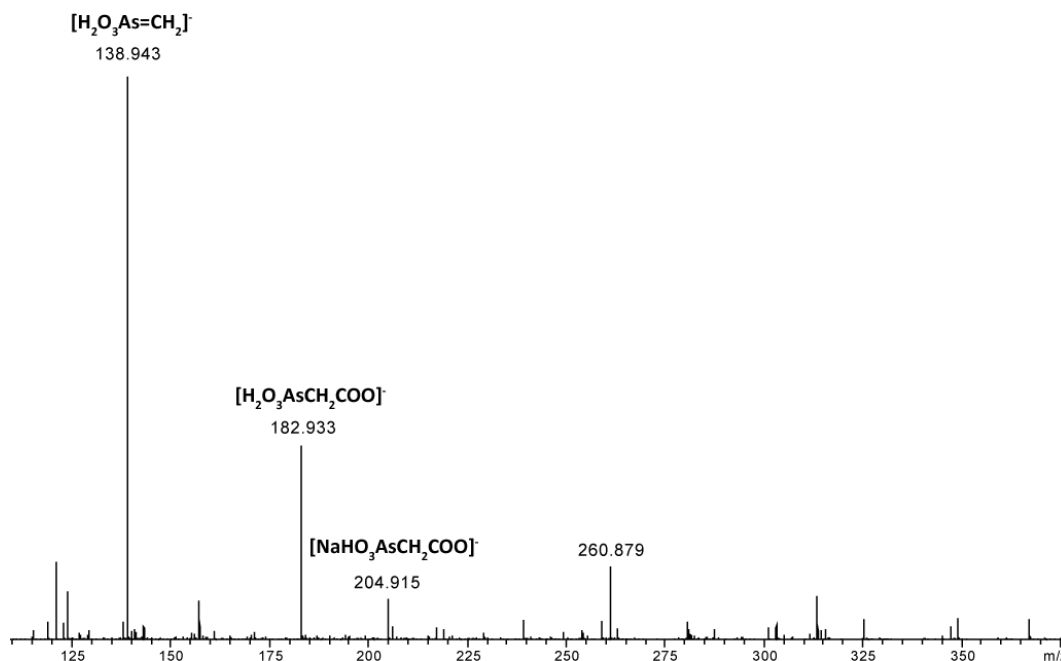


Figure 3.9 - HRMS of sodium arsonoacetic acid in H₂O, negative ion mode

The peaks in the mass spectrum of the sodium salt are not as readily assigned as they are for arsonoacetic acid. The major peak can be assigned to the ylide type fragment in which the carboxyl group is lost $[\text{H}_2\text{O}_3\text{As}=\text{CH}_2]^-$ (*m/z* 138.943), one of the smaller peaks seen in the spectrum of the free acid. The next largest peak is from the free acid, $\text{H}_2\text{O}_3\text{AsR}^-$ (*m/z* 182.993), where $\text{R} = \text{CH}_2\text{COO}^-$. It is only in one of the minor peaks we can see an ion associated with sodium, where one hydrogen has been exchanged to give $\text{NaHO}_3\text{AsR}^-$ (*m/z* 204.95). Also visible, although small are the $[(\text{H}_2\text{O}_3\text{AsR})_2+\text{H}]^-$ (*m/z* 366.863) and $[(\text{H}_2\text{O}_3\text{AsR})_2+\text{Na}]^-$ (*m/z* 388.845) ions. The ion at *m/z* 260 that was seen in the free acid, is also present here. It is once again able to be assigned the formula $[\text{C}_2\text{As}_2\text{H}_7\text{O}_5]^-$ (*m/z* 260.873), and likely to be from that of the ion shown in Figure 3.8.

3.1.6 Discussion of NMR results

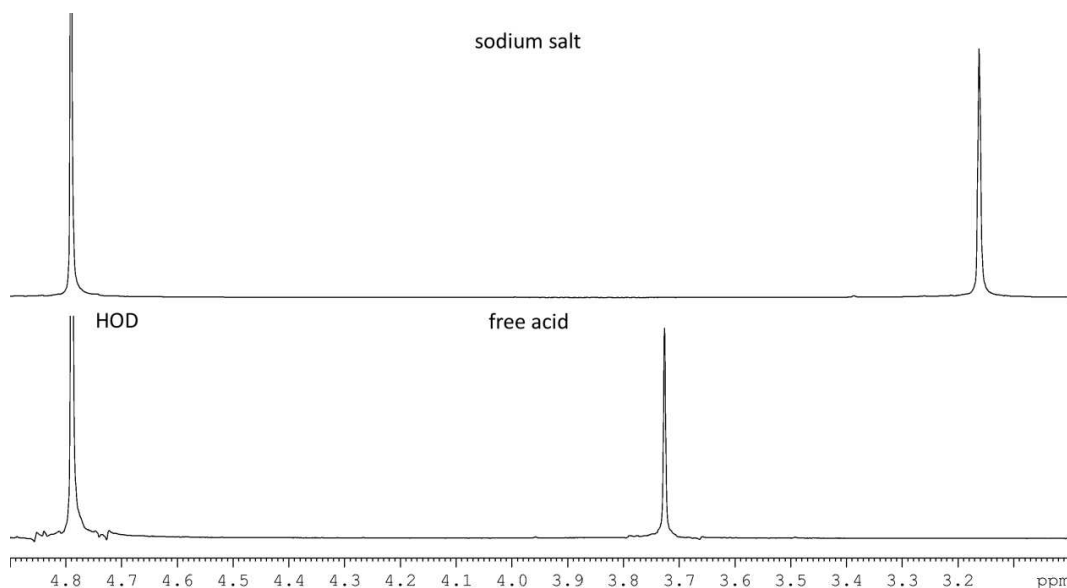


Figure 3.10 - ^1H NMR of the sodium salt and free acid of arsonoacetic acid (D_2O)

The ^1H -NMR spectrum of arsonoacetic acid and its salts in D_2O are very simple, showing only the CH_2 peak and the residual HOD solvent peak. No spectrum could be obtained of the barium salt because of its very poor solubility.

The spectra could be used as in an indicator of purity, as other products (containing hydrogen atoms) would be clearly seen. The free acid CH_2 peak is seen at 3.73 ppm, and the sodium salt more upfield at 3.16 ppm.

The change in chemical shift is much larger here than is seen in the ^1H spectra of similar set of compounds, acetic acid and sodium acetate. The sodium acetate CH_3 peak (1.92 ppm) moves upfield from the corresponding acetic acid peak (2.10 ppm) by 0.18 ppm. The sodium arsonoacetic acid CH_2 peak moves upfield from the free acid by 0.56 ppm.

The large change in chemical shifts must be able to be explained by the difference in structures. Arsonoacetic acid contains more groups able to carry charge than acetic acid, the carboxylate group, and the arsonic acid group. With the likelihood of more charged molecules in solution, electron density

can be withdrawn from the surrounding hydrogen, deshielding them, moving their signals further downfield.

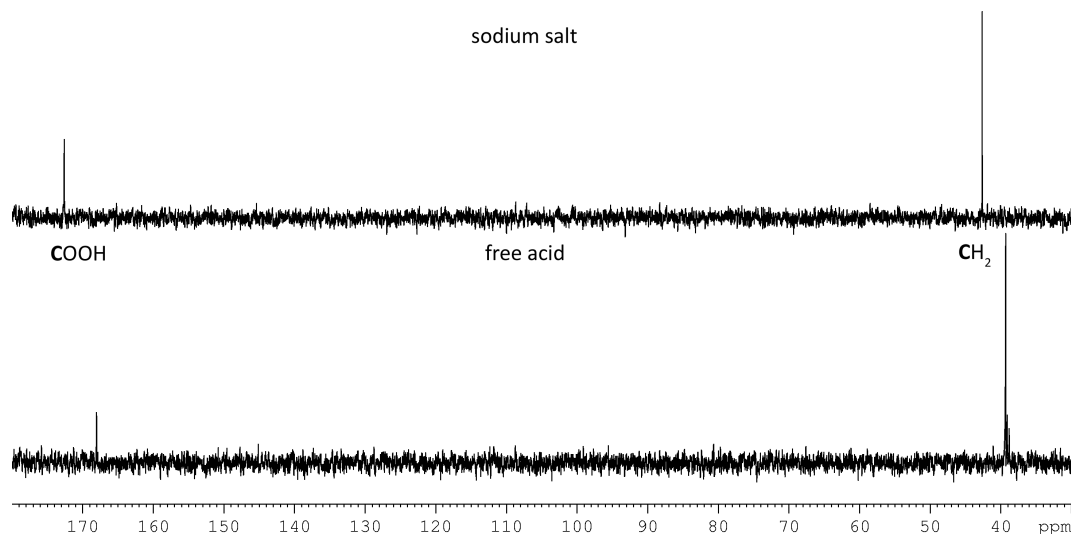


Figure 3.11 - ^{13}C NMR of sodium salt and free acid of arsonoacetic acid (D_2O)

The ^{13}C NMR spectra are also simple and readily assigned to the CH_2 and COOH carbons. The chemical shifts of the sodium salt peaks are slightly further downfield than those of the free acid; the COOH and CH_2 by 4 and 3 ppm respectively. Unlike the ^1H NMR, this is consistent with what is seen in the ^{13}C NMR spectra of acetic acid and sodium acetate, assumedly because the carbons are not involved in hydrogen bonding.

3.2 Arsenoacetic acid

3.2.1 Synthesis

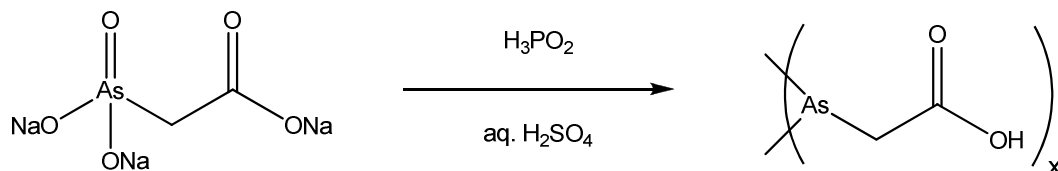


Figure 3.12 – Reaction scheme for arsenoacetic acid

Arsenoacetic acid was synthesised by reducing sodium arsonoacetic acid in a strongly acidic solution over a period of 3-5 days, using H_3PO_2 as the reducing agent. Palmer⁴⁰ used sodium hypophosphite (NaH_2PO_2), however this was not available, and H_3PO_2 provided comparable results. The orange precipitate was filtered after day three and the filtrate was left a further two days at which time a second crop could be filtered. The product was washed in water, in which it is practically insoluble.

If the product was left in solution longer, it began to darken and significant signs of impurities were seen in the mass spectrum. Palmer attributes this to the formation of ‘inorganic arsenic’ compounds and polyarsenide species.³⁷

The product is soluble in dilute sodium hydroxide as well as in pyridine. When dissolved in sodium hydroxide however, the colour of the solution changes within 1-2 hours, from an orange to a colourless solution, indicating breakdown. Crystals of X-ray quality were grown in a pyridine solution and stored over a period of weeks with no sign of degradation. The crystals did however decompose upon loss of solvent.

3.2.2 Discussion of X-ray crystal structure of cyclohexaarsenoacetic acid

A definitive structure of cyclohexaarsenoacetic acid was determined by means of X-ray crystallography, shown in Figure 3.13. Attempts to obtain crystals of other ring sizes were not successful.

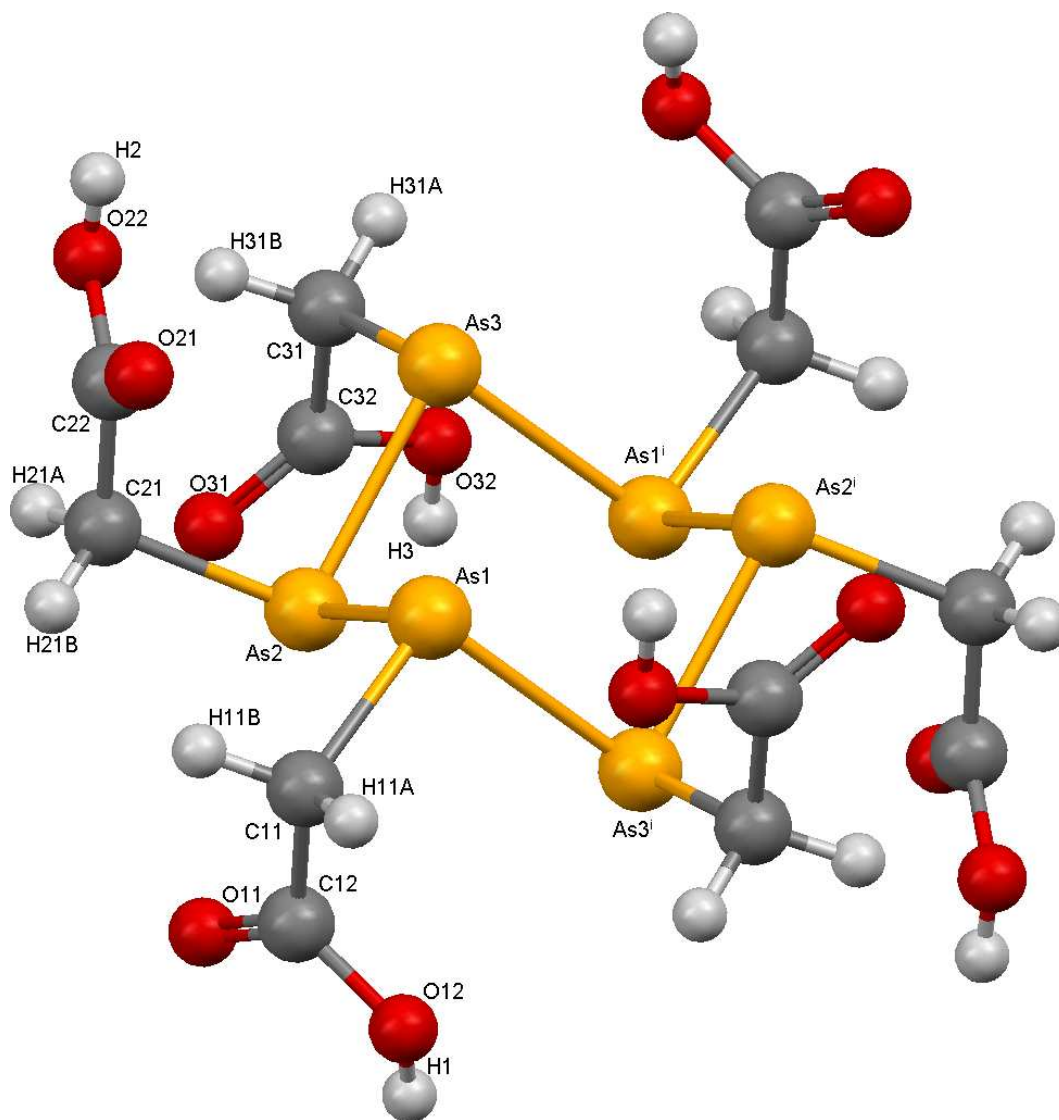


Figure 3.13 – The structure and labelling scheme of cyclohexaarsenoacetic acid (pyridine solvate molecules omitted for clarity). Only half the molecule is labelled, as the other half is generated by a crystallographic inversion centre

Table 3.4 - Selected bond lengths and angles for cyclohexaarsenoacetic acid

Bond lengths (Å)		Bond angles (°)	
As1-As2	2.4566(3)	As2-As1-As3 ⁱ	88.753(8)
As1-As3 ⁱ	2.4628(3)	As1-As2-As3	89.228(9)
As2-As3	2.4589(3)	As2-As3-As1 ⁱ	87.856(9)
As1-C11	1.9994(19)	C11-As1-As2	97.92(5)
As2-C21	1.9969(18)	C21-As2-As3	99.52(6)
As3-C31	2.0006(18)	C31-As3-As1 ⁱ	99.19(6)
O11-C12	1.216(2)	O11-C12-O12	124.27(17)
O12-C12	1.324(2)	O21-C22-O22	122.75(18)
O21-C22	1.220(2)	O31-C32-O32	124.10(18)
O22-C22	1.336(2)		
O31-C32	1.215(2)		
O32-C32	1.332(2)		

Symmetry transformations used to generate equivalent atoms:

(i): -x+2, -y+1, -z+1

There are only eight unique cycloarsenic compounds on the Cambridge Crystal Database⁶² with simple R substituents. The three hexacyclic compounds all have aromatic substituents, making cyclohexaarsenoacetic acid the first crystallised hexacyclic arsenic compound with only aliphatic substituents. Cyclohexaarsenoacetic acid exhibits many of the same characteristics as previously reported cyclic arseno compounds.

Cyclohexaarsenoacetic acid crystallises in the *P* $\bar{1}$ space group, with one acid molecule and six pyridine molecules in the unit cell (Figure 3.14). Because of the symmetry present, only half of the unit cell is unique.

The average As-As bond length is 2.459 Å, consistent with the crystal structure of (AsPh)₆, and the typical average As-As bond of 2.459 Å described by Rheingold.⁵² The ring is in a slightly more puckered chair conformation than (AsPh)₆ with an average As-As-As angle of 88.6° compared to 91.0°. All substituents are in equatorial positions. The C=O twists away slightly from the ring; the plane running through O-C-O is not exactly perpendicular to the As-C bond. The average angle of this twist is 4.2°.

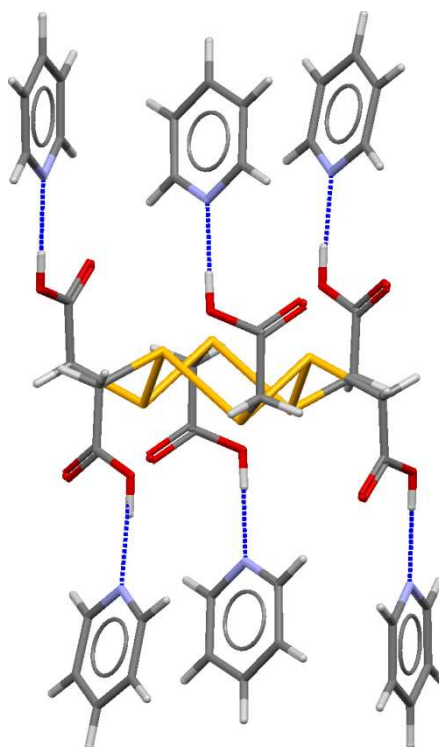


Figure 3.14- Structure of cyclohexaarsonoacetic acid with the six hydrogen bonded pyridine solvate molecules

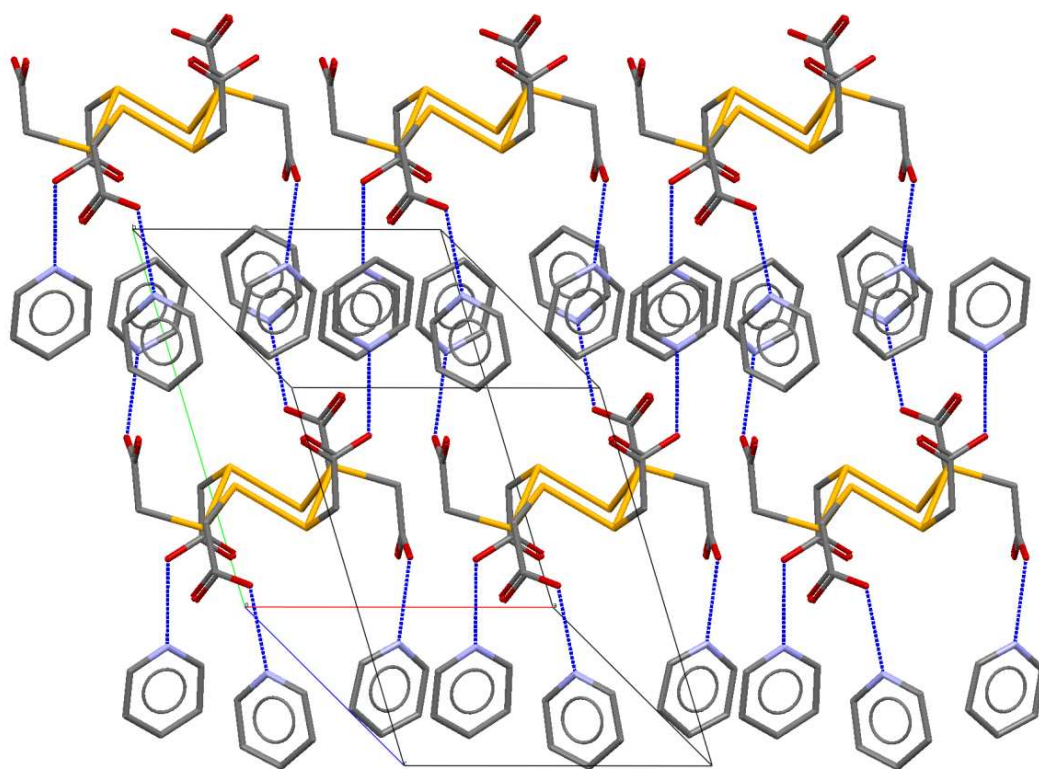


Figure 3.15 – Crystal packing diagram of cyclohexaarsonoacetic acid showing hydrogen bonds to pyridine molecules. Hydrogen atoms are omitted for clarity

Table 3.5 - Hydrogen bonds for cyclohexaarsenoacetic acid (Å and °)

D-H \cdots A	d(D-H)	d(H \cdots A)	d(D \cdots A)	<(DHA)
O12-H1 \cdots N5 ⁱ	0.85(3)	1.74(3)	2.585(2)	178(3)
O22-H2 \cdots N4 ⁱⁱ	0.82(3)	1.84(3)	2.658(2)	178(3)
O32-H3 \cdots N6 ⁱⁱⁱ	0.89(3)	1.74(3)	2.630(2)	172(3)

Symmetry transformations used to generate equivalent atoms:

(i): x, y+1, z; (ii): -x+1, -y, -z+1; (iii): -x+2, -y+2, -z+2

The hydrogen bonding in this crystal structure occurs between the carboxyl groups of the acid and the pyridine solvate molecules situated above each group. This encourages the formation of alternating layers of the acid, and pyridine molecules (Figure 3.15). The hydrogen position was refined and found within O-H bond distance, making it an O-H \cdots N hydrogen bond, rather than an O \cdots H-N pyridinium ion.

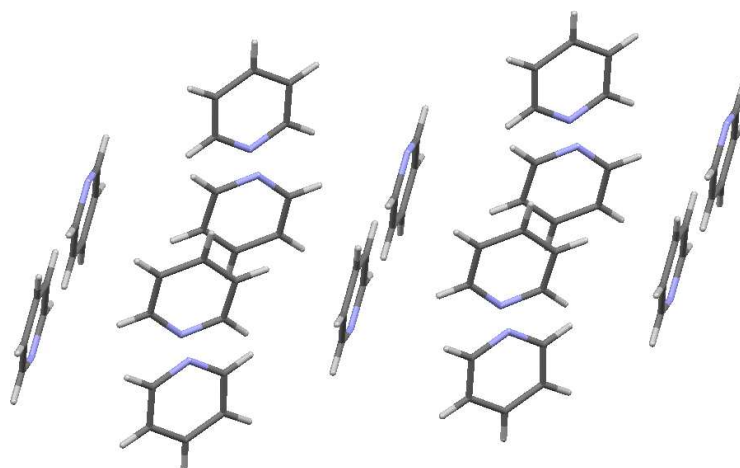


Figure 3.16 - Structural diagram showing the stacking of a layer of pyridine molecules in the cyclohexaarsenoacetic acid crystal structure

The H \cdots N distance is relatively short, indicating a strong hydrogen bond. O12-H1 \cdots N5 and O32-H3 \cdots N6 are 0.13 Å shorter than the average H \cdots N distance reported in a review by Jeffrey.⁷⁰ The hydrogen bonding forces the pyridine molecules to pack together relatively closely, with approximately 3.7 - 3.9 Å between adjacent molecules. Weak noncovalent π - π stacking interactions occur at these lengths.⁷¹ Energy minimisation calculations have been done with benzene molecules, and the lowest configurations were parallel stacking, and also a T-shape, where one molecule is perpendicular to

the other.⁷¹ Both types of interactions occur within this crystal structure between the pyridine molecules.

The X-ray crystal structure of cyclohexaarsenoacetic acid provides definitive evidence of the proposed cyclic structure of arsenoacetic acid. In keeping with previously determined cycloarsenic structures, the arsenic forms a puckered ring, with all substituents in equatorial positions. Further evidence for this structure is discussed in the following sections, with the hindsight of this data.

3.2.3 Discussion of FT-IR results

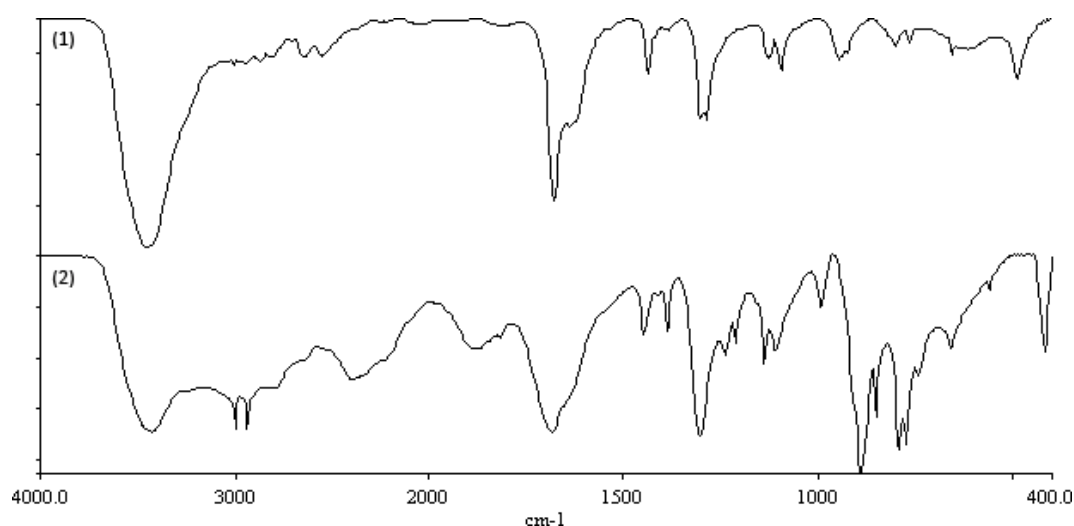


Figure 3.17 - FT-IR spectrum of (1) arsenoacetic acid, (2) arsonoacetic acid

Arsenoacetic acid and its precursor arsonoacetic acid share many peaks as one would expect. The major peaks are summarised and compared below in Table 3.6.

Table 3.6 - Summary and comparison of FT-IR data for arsono- acid and arsono- acetic acid (cm^{-1})

	Arsenoacetic acid (1)	Arsonoacetic acid (2)
OH stretch (broad)	3300-3700 (vs)	3300-3700 (s)
C=O stretch	1681 (s)	1683 (s)
CH ₂ bending and scissoring	1439 (m)	1448 (m)
	1384 (w)	1388 (m)
C-O stretch	1303 (s)	1303 (s)

(w) = weak, (m) = medium, (s) = strong, (vs) = very strong

There is a very close correlation between the two spectra, the maximum difference being 9 cm^{-1} for one of the CH_2 bending modes. The $\text{As}=\text{O}$ stretches at about 890 cm^{-1} , present in arsonoacetic acid and its salts, are absent from arsonoacetic acid, which is a good initial confirmation that arsonoacetic acid has been reduced, and now only forming As-As or As-C bonds. Also absent in the spectrum of arsonoacetic acid, is the very broad band from $3800\text{--}2000 \text{ cm}^{-1}$ caused by the strong intermolecular hydrogen bond network present in arsonoacetic acid.

3.2.4 Discussion of HRMS results

The mass spectrum of arsonoacetic acid is so far the only indication that various sized cyclic structures $(\text{RAs})_n$ exist together in solution.

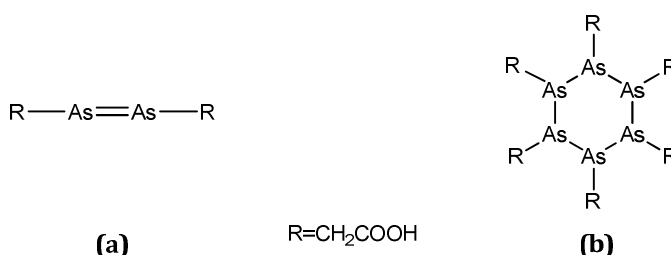


Figure 3.18 - Diagram showing (a) Palmer's original diarsene structure of arsonoacetic acid, (b) newly proposed cyclic structure

Palmer, who synthesised arsonoacetic acid initially, assigned the compound as a diarsene (Figure 3.18a).³⁷ By analogy with the recent work done on

Salvarsan by Lloyd *et al.*, it seems likely that rather than a simple diarsene compound, multiple cyclic compounds are present in the one solution.¹⁷ The evidence for this can be seen below in Figure 3.19. The addition of pyridine to deprotonate the acid was required before a spectrum could be seen.

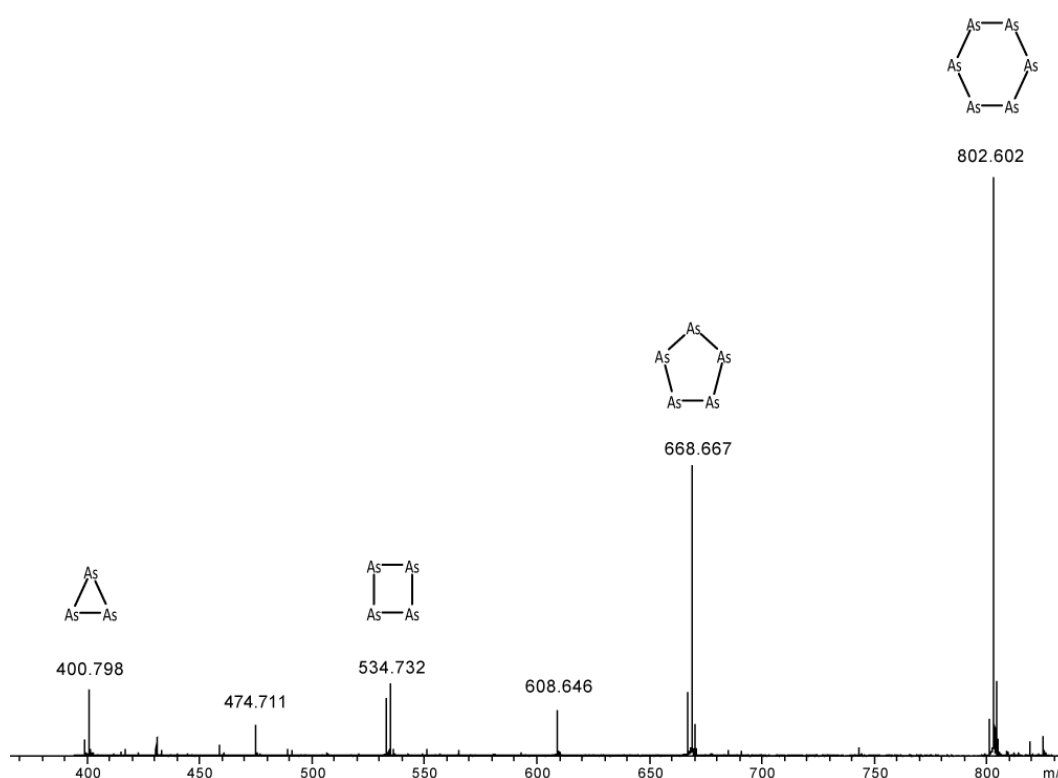


Figure 3.19 - HRMS of arsenoacetic acid in H₂O, m/z 400-850, negative ion mode (ring substituents off each As have been left off for clarity)

The series $[(\text{RAs})_3\text{-H}]^-$, $[(\text{RAs})_4\text{-H}]^-$, $[(\text{RAs})_5\text{-H}]^-$ and $[(\text{RAs})_6\text{-H}]^-$ are present as the four main peaks, where R = CH₂COOH. Upon closer inspection at higher masses, the series can be seen continuing up to $[(\text{RAs})_{11}\text{-H}]^-$. Peaks exactly 2.02 Da lower than the $[(\text{RAs})_n\text{-H}]^-$ ions are present all the way through the spectrum, the mass of exactly two hydrogen atoms. The exact arrangement is unknown, however it is possible that two substituents are forming an As=C bond, where previously there was only a single bond. Only the -2H peak is seen, and no other combinations which is unusual.

It has been suggested previously that only one species is present in solutions of cycloarsenic compounds, and the observed mass spectrum is a

combination of fragment ions and aggregates.³⁶ This is most likely true for spectra obtained using electron impact (EI) ionisation. This is a much harsher ionisation technique than the electrospray ionisation (ESI) source present in the MicrOTOF. ESI has been shown to be a soft ionisation technique, not leading to significant fragmentation, making it ideal for speciation studies as M^+ parent ions are usually seen.^{72, 73}

When varying the cone voltage, the relative intensities of the peaks for arsenoacetic acid only change slightly. If the smaller rings were caused by fragmentation, you would expect a significant change under different conditions, suggesting the presence of multiple cyclic species. Lloyd *et al.* also carried out MS/MS studies whereby fragmentation was deliberately induced. No sign of smaller ring sizes forming from the larger were present, only R , R_2As , and R_3As fragments.¹⁷

The water soluble sodium salt of arsenoacetic was also synthesised, the HRMS is shown below in Figure 3.20. Like the free acid, the addition of pyridine was required to see a mass spectrum of the sodium salt. This seems unusual as the presence of sodium will increase the pH of the solution, which should deprotonate the acid without the addition of a base.

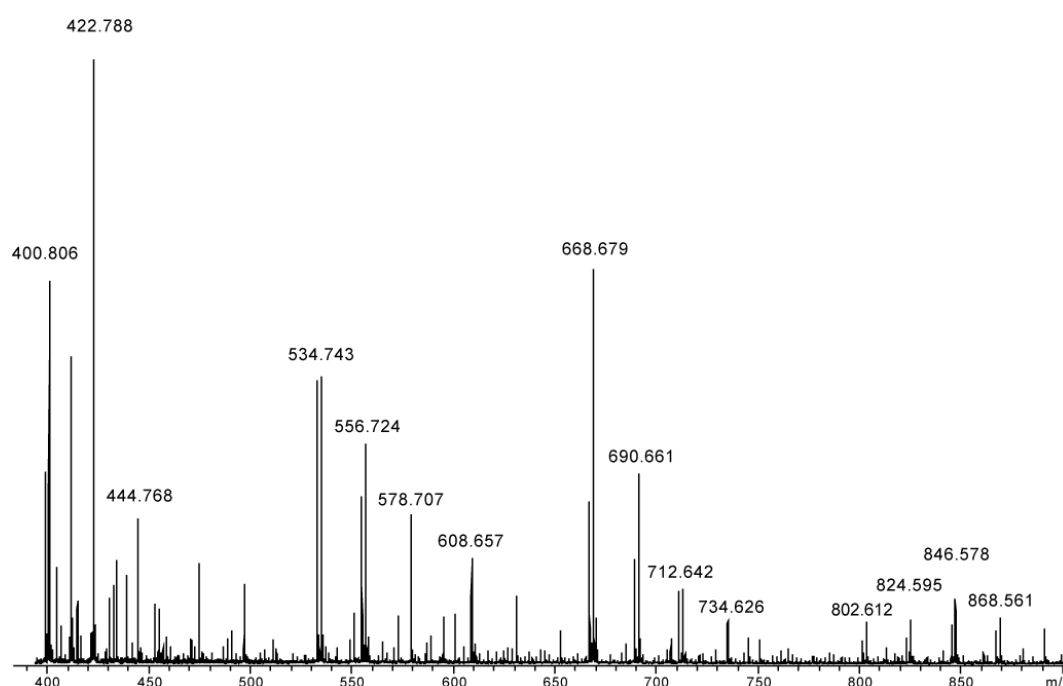
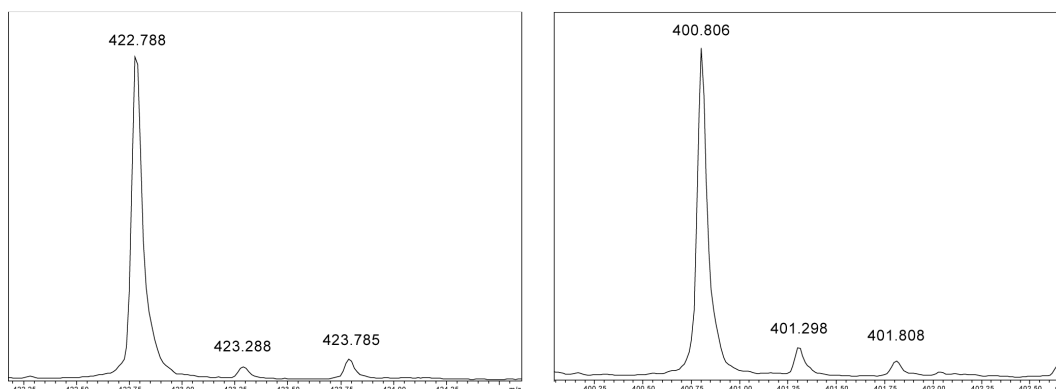


Figure 3.20- HRMS of sodium arsenoacetic acid in H_2O , negative ion mode

Table 3.7 - Peak assignment for the HRMS of sodium arsenoacetic acid (Figure 3.20)

Ion	<i>m/z</i>	Ion	<i>m/z</i>
$[(\text{AsR})_6+3\text{Na}^+-4\text{H}^+]\cdot$	868.561	$[(\text{AsR})_4+3\text{Na}^+-4\text{H}^+]\cdot$	600.69
$[(\text{AsR})_6+2\text{Na}^+-3\text{H}^+]\cdot$	846.578	$[(\text{AsR})_4+2\text{Na}^+-3\text{H}^+]\cdot$	578.707
$[(\text{AsR})_6+\text{Na}^+-2\text{H}^+]\cdot$	824.598	$[(\text{AsR})_4+\text{Na}^+-2\text{H}^+]\cdot$	556.724
$[(\text{AsR})_6-\text{H}^+]\cdot$	802.612	$[(\text{AsR})_4-\text{H}^+]\cdot$	534.743
$[(\text{AsR})_5+3\text{Na}^+-4\text{H}^+]\cdot$	734.626	$[(\text{AsR})_3+2\text{Na}^+-3\text{H}^+]\cdot$	444.768
$[(\text{AsR})_5+2\text{Na}^+-3\text{H}^+]\cdot$	712.642	$[(\text{AsR})_3+\text{Na}^+-2\text{H}^+]\cdot$	422.788
$[(\text{AsR})_5+\text{Na}^+-2\text{H}^+]\cdot$	690.661	$[(\text{AsR})_3-\text{H}^+]\cdot$	400.806
$[(\text{AsR})_5-\text{H}^+]\cdot$	668.679		

Although complex, most peaks can be readily assigned. The same $[(\text{RAs})_n-\text{H}]\cdot$ ($n = 3-6$) series present in the arsenoacetic acid spectrum are present here. The relative intensities of the different ring sizes appear to be different from that of the free acid.

**Figure 3.21- Isotope patterns of the 422.788 and 400.806 Da ions in the sodium arsenoacetic acid mass spectrum**

It appears that the three-membered ring is the most abundant, contradictory to the free acid, however upon closer inspection, two of the peaks (m/z 422.788 and 400.806) are disproportionately larger than the other ions associated with the three-membered ring. They also have isotope patterns with 0.5 Da increments, indicative of a $2\cdot$ ion. The higher pH generated by sodium may encourage the formation of multiply charged ions more so than the free acid.

From the isotope pattern we can calculate that 32% of the 422.788 Da signal is from $[(\text{RAs})_6+\text{Na}-3\text{H}]^{2-}$, and 70% of the 400.806 Da signal is from $[(\text{RAs})_6-2\text{H}]^{2-}$. Even with the contributions from these peaks, it appears the six-membered ring is still not as abundant as in the free acid. It is possible that more highly charged ions are present, contributing to an even greater percentage of ions attributed to the six-membered ring, however mass spectral data was not obtained below 400 Da, excluding these peaks.

Also present are the series of ions, whereby one, two, or three of the hydroxyl hydrogen atoms have been replaced by sodium. This gives the series $[(\text{RAs}-\text{H}+\text{Na})_n-\text{H}]^-$, $[(\text{RAs}-2\text{H}+3\text{Na})_n-\text{H}]^-$, and $[(\text{RAs}-3\text{H}+3\text{Na})_n-\text{H}]^-$. Ions with more than three sodium atoms are not seen, even for the larger ring sizes. The degree to which sodium has replaced the hydroxyl hydrogen atoms in the salt cannot be identified from this spectrum because of the equilibria the acid undergoes in solution. It could be assumed that even if only some of the hydroxyl hydrogen atoms were exchanged, the product would still be water soluble.

Data obtained for both arsenoacetic acid and its sodium salt provide evidence for the presence of multiple cyclic structures in solution, where once a diarsene structure was proposed.

3.2.5 Discussion of NMR results

The ^{13}C spectra of arsenoacetic acid and its precursor arsonoacetic acid are shown in Figure 3.22. The acetic acid group gives rise to the two peaks present in both compounds, and the chemical shifts of both compounds vary only a little. Although an indication of their similar chemical environments, direct comparisons cannot be made because of solvent effects. Arsenoacetic acid was run in pyridine- d_5 and arsonoacetic acid in D_2O .

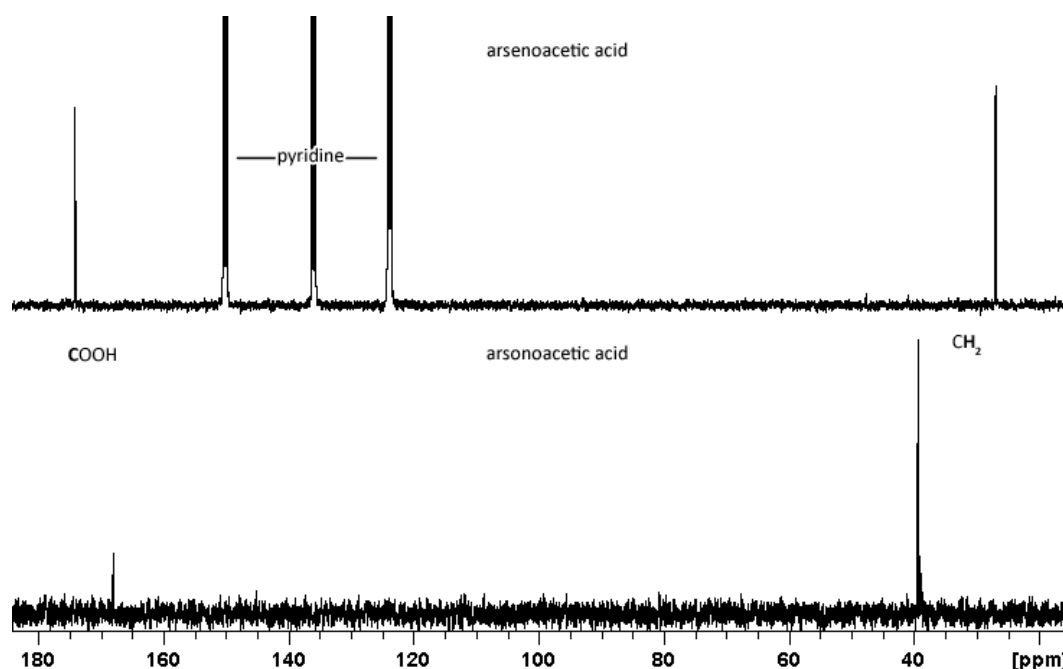


Figure 3.22- ^{13}C NMR data comparing arsonoacetic (pyridine- d_5) and its precursor arsonoacetic acid (D_2O)

Both the ^1H (Figure 3.23) and ^{13}C (Figure 3.24) NMR spectra of arsonoacetic acid are very simple, and not particularly useful for the characterisation of arsonoacetic acid. However, resolution enhancement of the CH_2 peak, directly bonded to the arsenic ring, were carried out in hope of gaining more insight into the presence of multiple cycloarsenic structures of varying sizes in solution.

In organic systems, different sized rings have been well studied, and was shown to have a significant effect on the chemical shift of an exocyclic carbonyl group because of ring strain.⁷⁴ The ^{13}C CH_2 peak in ethylcyclohexane and ethylcyclopentane come at 30 and 29 ppm, the ^1H at 0.85 and 0.90 ppm respectively.

A group studying cycloantimony and -bismuth rings with $(\text{Me}_3\text{S}_2)\text{CH}$ groups were able to identify different ring sizes an equilibrium mixture of R_3Bi_3 and R_3Bi_4 in the ^1H NMR, seeing separation for both the CH_3 and CH proton signals.⁷⁵

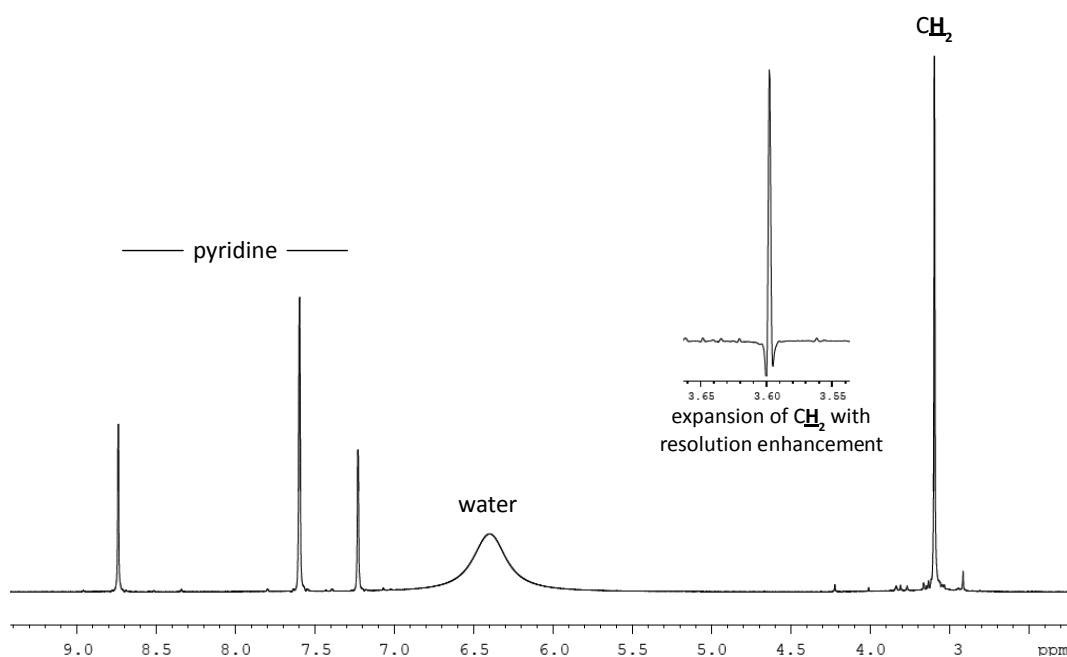


Figure 3.23 – ^1H NMR spectrum of arsenoacetic acid ($\text{pyridine-}d_5$) with expansion and resolution enhancement of CH_2 peak

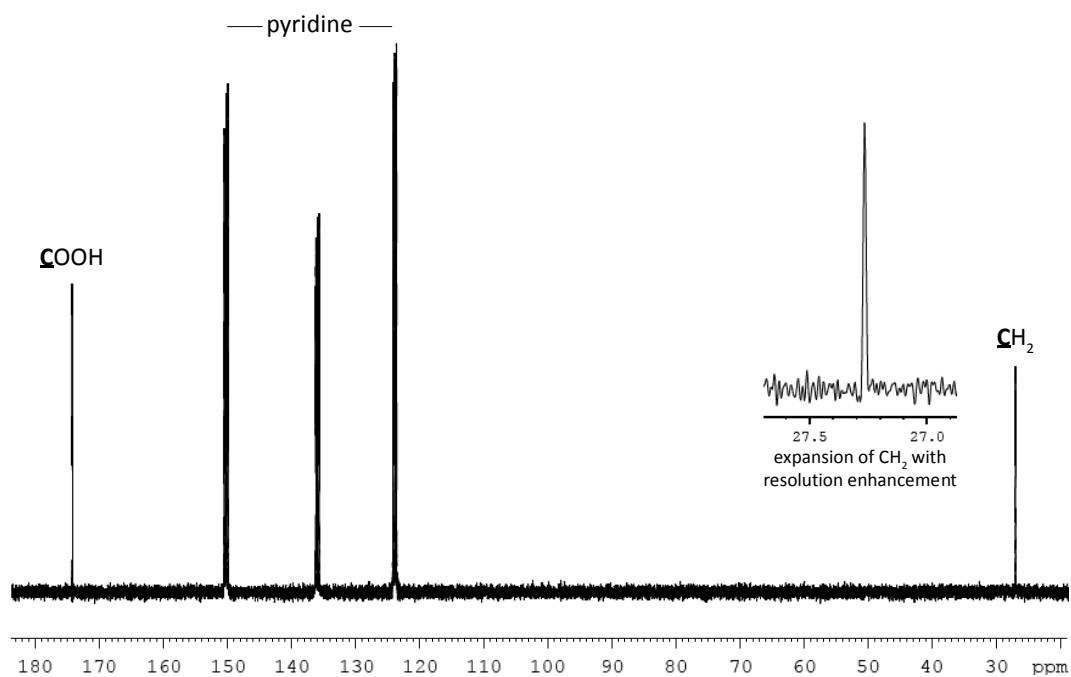


Figure 3.24 – ^{13}C NMR spectrum of arsenoacetic acid ($\text{pyridine-}d_5$) with expansion and resolution enhancement of CH_2 peak

Although all cases are different to that of arsenoacetic acid, clear analogies can be seen. In the case of arsenoacetic acid, we assumed that the CH₂ bonded to the arsenic ring would have a slightly different chemical shift, depending on the size of the ring they are bonded to. Therefore, if there were multiple molecules, varying in ring size in solution, we would see either multiple peaks, or a broadening of the peak if the chemical shifts were very close.

There are no signs of multiple peaks, or broadening of the ¹H peak (Figure 3.23), nor for the equivalent ¹³C peak (Figure 3.24), even after applying resolution enhancement. The protons giving rise to this peak are two bonds away from the ring itself, this could be too far away to observe the effect; the carbon atom however is attached directly to the ring.

Two scenarios could explain this. Firstly, the sharpness of the peak could indicate that only one ring size is present in solution. A crystal was grown in pyridine and the structure determined to be that of the six-membered cycloarsenoacetic acid. With those two pieces of data, it could be said that only cyclohexaarsenoacetic acid is present in a pyridine solution. The second possible explanation is less likely, however if there were multiple ring sizes rapidly interconverting between one another, a sharp peak would also be seen.

3.2.6 Attempted separation of rings using HPLC

An attempt was made to separate out the series of cycloarsenic structures using HPLC with an anion exchange column. The separation and identification of arsenic speciation has been carried out previously with great success using anion exchange HPLC.^{76, 77}

Using a basic solvent, each acetic acid group should carry a negative charge which will interact with the column. The six-membered ring will have more negative charge than the five-membered ring, which has more negative charge than the four-membered ring etc., hopefully being sufficient to separate each ring size. The fractions would then be collected and analysed using HRMS.

Separation proved to be more difficult than anticipated. For practical purposes, sodium hydroxide was used as the base, however arsenoacetic acid appears to degrade in this solution over a period of 1 – 2 hours, changing from orange to colourless. With HPLC runs of 40 mins this would be sufficient time to collect fractions and still see the intended peak in the mass spectrum. The TIC of a run using sodium hydroxide as the base is shown in Figure 3.25.

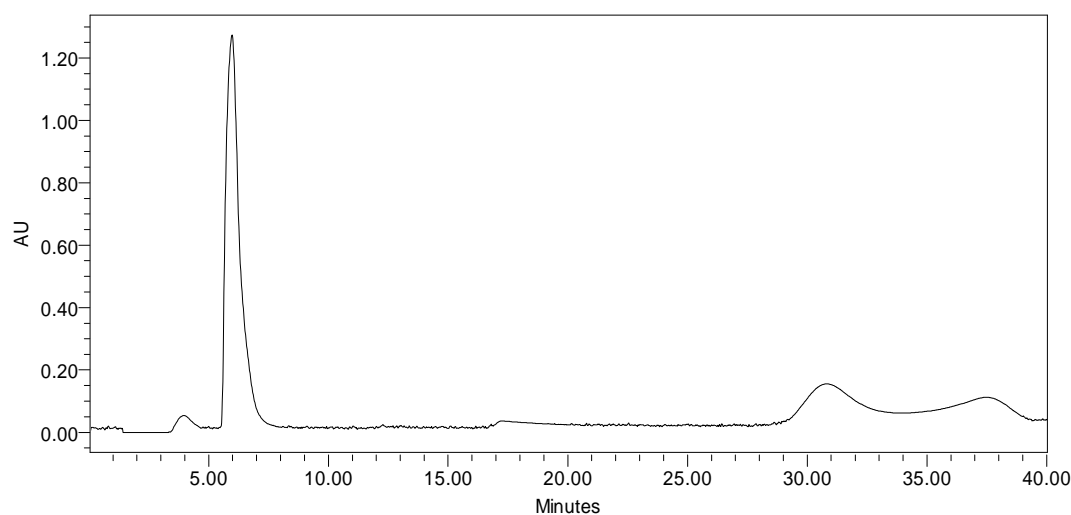


Figure 3.25 –HPLC max plot of arsenoacetic acid in 5:95 MeCN:H₂O, 50 mmol NaOH (190 – 400 nm)

There are four clearly visible peaks and one small 'hump' visible in the TIC where sodium hydroxide was used, all having a λ_{max} at 214 ± 2 nm. The two peaks eluting last also have a shoulder occurring ~ 235 nm giving them a much broader UV spectrum. Smaller ring sizes would elute first, however from the UV data it is impossible to say which compound has eluted when, or if separation has occurred at all. During the 40 minute run, it is likely that degradation has occurred to some degree because of the sodium hydroxide. It is possible the peaks seen could be various degradation products with similar UV spectra. In the UV-Vis spectrum of the crude arsenoacetic mixture, the shoulder peak at ~ 235 nm was seen, however it was more defined. Since the UV-Vis spectrum was obtained much quicker than that from HPLC, is it possible that the lack of definition of this peak indicates degradation.

Fractions were collected and analysed by mass spectrometry but no peaks were seen.

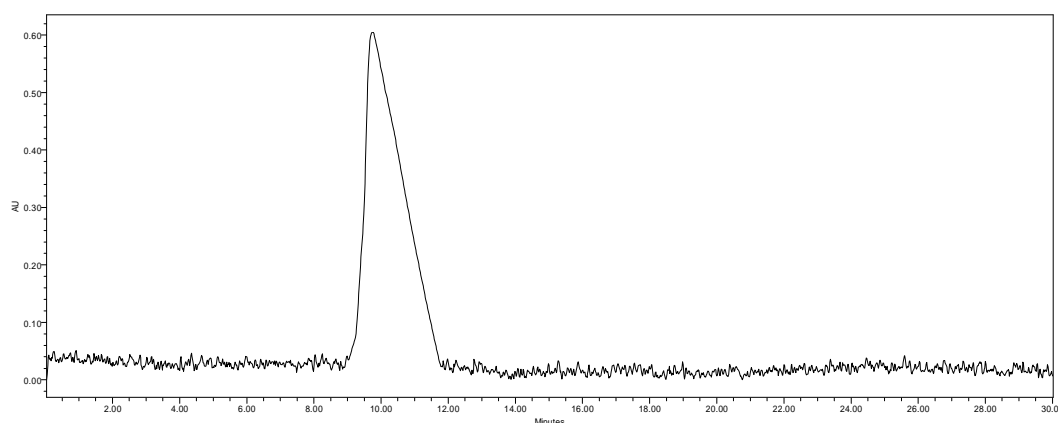


Figure 3.26 –HPLC max plot of arsenoacetic acid in 5:95 MeCN:H₂O, 40 mmol pyridine (190 – 400 nm)

Pyridine was also tried as a base giving a very different result (Figure 3.26). No sign of separation was seen. Since pyridine is a weaker base than sodium hydroxide, it is possible that not all acetic acid groups had a negative charge. It was still assumed that the larger ring sizes would overall be more negatively charged than their smaller counterparts. As seen in the solid state by X-ray crystallography (Section 3.2.2), the pyridine molecules merely hydrogen bond to the carboxyl hydrogen, rather than forming a pyridinium ion and a negatively charged carboxyl group. This could be the same case in solution, where the pyridine aids in the solubility of arsenoacetic acid, but does not create the negative charge required for separation in an anionic exchange column, potentially explaining why only one broad peak is seen eluting. By increasing the concentration of pyridine from 40 to 100 mmol, the broad peak elutes 3 minutes earlier (from 9 to 6 min) and there is a loss of sensitivity from the UV detector because of the increased intensity of pyridine in the solvent. A sample from this broad peak shows the original mass spectrum containing peaks from multiple ring sizes.

Also worthy of mention is the difference in the λ_{max} measured using the two different bases, 214 nm in the sodium hydroxide solution and 272 nm in the pyridine solution. The λ_{max} of an acetate group is ~ 208 nm⁷⁸, so it is likely that the 214 nm chromophore in the sodium hydroxide solution, is from the carboxylate group in arsenoacetic acid. The 272 nm wavelength observed in

the pyridine solution lies within the range typically seen for pyridinium cations. It is possible that this is what we are seeing here.

The pyridine is the only thing keeping arsenoacetic acid in solution, as it is practically insoluble in water, and so the interactions between pyridine and the acid will be relatively strong. Even though in the crystal structure of cyclohexaarsonoacetic acid we see a pyridine molecule hydrogen bonded to the acid, in solution the pyridine molecules may carry a slight charge, and give rise to this particular wavelength. Even if it is the pyridinium ion we are detecting, rather than the acid itself, it can still be used to identify when arsenoacetic acid elutes. If the peak we see elutes from 9-12 minutes, this is the time at which arsenoacetic acid is eluting, as it is the only time the pyridinium ion exists because of the interactions with the acid. This still indicates that no separation has occurred in the anion exchange column.

3.2.7 Attempted esterification of arsenoacetic acid, NMR spectroscopy and GC-MS results

An attempt to synthesise the methyl ester of arsenoacetic acid was made in hope of making a compound able to be run directly on a GC or reverse phased HPLC column.

Direct esterification was attempted by stirring arsenoacetic acid in methanol, however because of the poor solubility of arsenoacetic acid, no reaction took place, even after stirring for 24 hours.

Making the methyl ester P^{I} the acid chloride was then attempted. Arsenoacetic acid was added to thionyl chloride, and a few drops of pyridine under N_2 . McMurry⁶⁰ proposes that the pyridine speeds up the reaction by making more Cl^- available. Arsenoacetic acid did not dissolve in the thionyl chloride until the pyridine was added, so in this reaction it may just be necessary to dissolve the acid so that it is able to react. Initially it appeared that arsenoacetic acid would not dissolve in thionyl chloride, but on addition of pyridine, it dissolved instantly forming a dark orange solution. Once the evolution of SO_2 and HCl had stopped, the thionyl chloride was removed

under vacuum. Super dry methanol was added resulting in a bright yellow solution. Whilst in the methanol solution there were no visual signs of degradation even after months of storage.

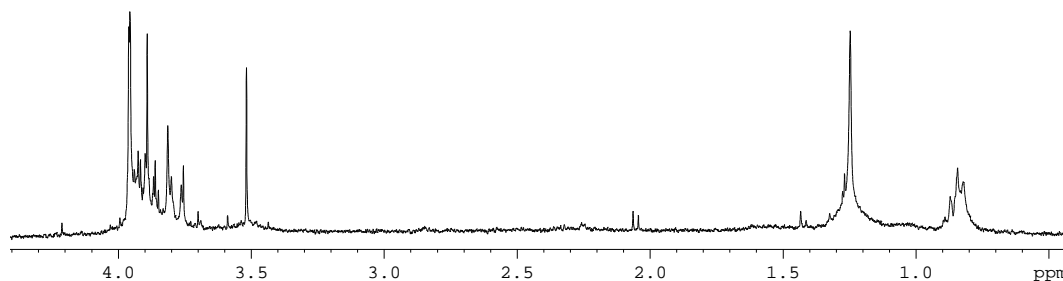


Figure 3.27 – ^1H NMR of crude solution from attempted esterification of arsenoacetic acid (CDCl_3)

The NMR spectrum of the crude product (Figure 3.27) shows that the methyl ester is not the only product to have formed, if at all. Peaks occur in the regions where we would expect the methylene protons (3.5 ppm) and the ester methyl protons (3.8 – 4.0 ppm), however there are also many other peaks in this region. Although it is possible the arsenoacetic acid methyl ester had formed, it could not be confirmed from this spectrum. The mass spectrum was also messy, and no identifiable peaks could be seen.

The crude yellow methanol solution was run on the GC, however only ions smaller than expected were seen. Palmer³⁷ observed decomposition of arsenoacetic acid at temperatures above 205 °C, however this temperature was not reached in the GC until after all peaks had eluted, ruling out thermal decomposition. The TIC can be seen below in Figure 3.28.

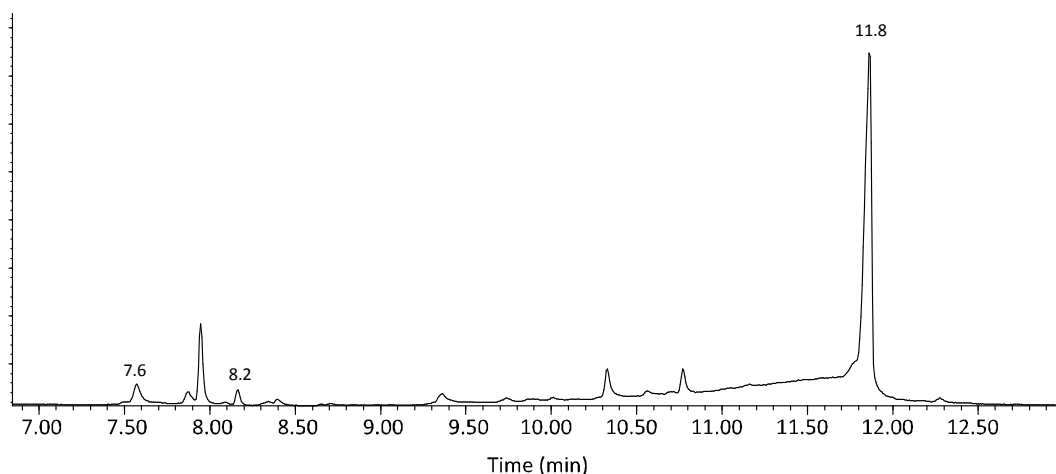


Figure 3.28 - TIC from GC-MS of crude methanol solution from the esterification of arsenoacetic acid

A large solvent front and fast eluting compounds could be seen up to 3.6 mins. A shoulder at the end of the peak revealed the presence of the relatively stable AsCl_3^+ fragment with an m/z of 180, most likely coming from the reaction with SOCl_2 .

Two of the peaks (7.6 and 8.2 mins) show three interesting fragments at m/z 59, 75 and 134, assigned COOCH_3^+ , As^+ and AsCOOCH_3^+ respectively. These are potentially fragments of an arsenoacetic acid ester. The peaks eluting at different times could be because of the presence of different ring sizes, or only some of the acetic acid groups being esterified.

From 11.0 – 11.8 mins, something can be seen slowly eluting off the column with a peak showing at 11.8 mins, this is typical of S_8 , S_6 and similar degradation products. This was the final peak to elute.

From these observations, it appears that the methyl ester can not be formed *via* the acid chloride pathway.

3.2.8 Discussion of X-ray crystal structure of β -monoclinic S_8 (β - S_8)

Serendipitously, crystals that had formed in the crude methanol solution were analysed by X-ray crystallography and determined to be sulfur, β - S_8 (Figure 3.29). This agrees with the sulfur peak seen in the previously discussed GC-MS data. It appears that arsenoacetic acid reduces SOCl_2 when

trying to synthesise the acid chloride, forming elemental sulfur and AsCl_3 , also identified in the GC-MS.

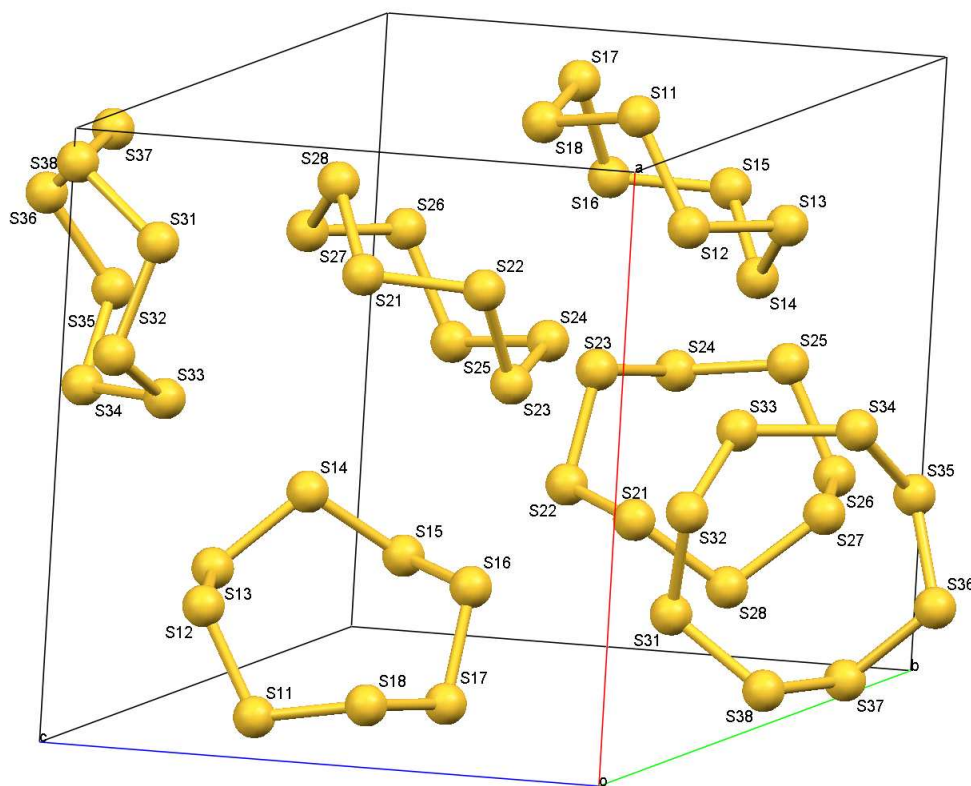


Figure 3.29 – Molecular diagram of β -monoclinic S_8 showing unit cell and labelling scheme. Note only half the molecules in the unit cell are unique

Although the β -monoclinic allotrope of S_8 that crystallised has previously been determined, it is said to be unstable with respect to the orthorhombic S_8 at temperatures below $95.3\text{ }^\circ\text{C}$.⁷⁹⁻⁸² Our solution was never heated above room temperature, and was also stored at room temperature. Previous attempts to crystallise the β form from molten sulfur have shown that if kept at room temperature, conversion to the polycrystalline orthorhombic sulfur occurs within the hour.⁸⁰ The enthalpy of the transition from α to β form is small (0.4 kJ mol^{-1} at $95\text{ }^\circ\text{C}$).⁸³

The reason for favouring the β -monoclinic allotrope under these conditions is unknown. A plausible explanation is that the oxidised arsenic, or any of the other impurities in solution may stabilise it, or make the α - S_8 less favourable somehow. It is not possible to determine exactly what was in the methanol

solution that may have caused this, but it is unambiguous that the conditions not only led to crystallisation of the high temperature phase at room temperature and the resulting crystals survived unchanged at room temperature for several months.

Previously, β -S₈ has only been prepared from molten sulfur. When crystallising, it is very likely that some of the α -S₈ allotrope also forms, although able to be separated visually. The presence of α -S₈ could act as a seed crystal for the conversion from the β -monoclinic form to the orthorhombic form. It is possible that from the methanol solution, only the β allotrope crystallised. The absence of any seeding α -S₈ crystals could explain why the β -S₈ survived so long at room temperature.

The unit cell consists of six S₈ rings in a crown conformation in the $P2_1$ space group. Only half of the rings in the unit cell are unique as the other half are generated by two screw axes.

An in-depth study by Goldsmith and Strouse revealed that at room temperature, β -S₈ exhibits space group symmetry $P2_1/c$. Of the six molecules in the unit cell, two are twofold disordered with an inversion centre.⁸¹ At temperatures below 198 K, the molecules become more ordered. The inversion centre and c glide plane vanish, resulting in a $P2_1$ space group as seen in this crystal structure.⁸¹

Twinning was seen in the room temperature crystal structure of β -S₈ reported by Templeton, whereby the directions of the a and b axes are reversed and so the structure was refined as a racemic twin.^{79, 80} The twinning appears to be present in this crystal structure as well. Templeton describes a pseudosymmetry that would allow the two different orientations to exist simultaneously at the twin boundary and if this symmetry were to be present throughout the entire crystal, it is suggested that it would exhibit ferroelastic properties.⁸⁰

The bond lengths and angles vary little. The bond lengths are 2.05 (\pm 0.01) Å and the angles, 107.8° (\pm 0.2).

4. Conclusions

The structure of arsonoacetic acid has been confirmed by means of X-ray crystallography, mass spectral data and NMR. The crystal structure was found to be isomorphous with the phosphorus analogue, phosphonoacetic acid.

Mass spectral data shows that arsenoacetic acid exists as a mixture of different sized cycloarsenic structures in solution, not as the diarsene structure that was first proposed, a characteristic first noticed by Lloyd *et al.* in Salvarsan.¹⁷ This is in agreement with today's understanding that As=As bonds only form when the substituents are very sterically crowded.²⁰

The structure of the six-membered arseno ring, cyclohexaarsenoacetic acid, has been determined without doubt by means of X-ray crystallography. Like previously reported cycloarsenic crystal structures, arsenoacetic acid forms a puckered arseno ring with all substituents in equatorial positions.

Although no other ring sizes could be isolated, this is not sufficient evidence to say that the other ring sizes are not present. Work done on cyclobismuth systems have resulted in definitive NMR data supporting the existence of a five-membered ring, yet crystal structures have only been obtained for the three- and four-membered rings.⁷⁵ Mass spectral data of the cyclobismuth compounds was not published. However in the present case, the lack of any broadening or splitting of the ^{13}C or ^1H signals is a puzzle if there are indeed varying ring sizes in the sample.

5. Appendix – Complete X-Ray Crystal Data

5.1 Arsonoacetic acid – $\text{H}_2\text{O}_3\text{AsCH}_2\text{COOH}$

Table 5.1 - Crystal data and structure refinement for arsonoacetic acid

Empirical formula	$\text{C}_2\text{H}_5\text{AsO}_5$
Formula weight	183.98
Temperature	93(2) K
Wavelength	0.71073 Å
Crystal system	Orthorhombic
Space group	$P2_12_12_1$
Unit cell dimensions	$a = 6.0904(3)$ Å $b = 7.7557(4)$ Å $c = 10.4713(5)$ Å
Volume	$494.62(4)$ Å ³
Z	4
Density (calculated)	2.471 Mg/m ³
Absorption coefficient	6.800 mm ⁻¹
F(000)	360
Crystal size	0.40 × 0.56 × 0.60 mm ³
Theta range for data collection	3.27 to 32.61°.
Index ranges	-8 ≤ h ≤ 8, -11 ≤ k ≤ 11, -15 ≤ l ≤ 15
Reflections collected	13348
Independent reflections	1764 [R(int) = 0.0548]
Completeness to theta = 32.61°	98.2 %
Absorption correction	Semi-empirical from equivalents
Max. and min. transmission	0.1718 and 0.1057
Refinement method	Full-matrix least-squares on F ²
Data / restraints / parameters	1764 / 0 / 76
Goodness-of-fit on F ²	1.188
Final R indices [I > 2σ(I)]	R1 = 0.0190, wR2 = 0.0507
R indices (all data)	R1 = 0.0192, wR2 = 0.0507
Largest diff. peak and hole	0.384 and -1.202 e Å ⁻³

Table 5.2 - Atomic coordinates ($\times 10^4$) and equivalent isotropic displacement parameters ($\text{\AA}^2 \times 10^3$) for arsonoacetic acid. U(eq) is defined as one third of the trace of the orthogonalized U^{ij} tensor

	x	y	z	U(eq)
As(1)	8947(1)	2781(1)	6528(1)	8(1)
C(1)	6659(3)	1721(2)	7514(2)	11(1)
C(2)	6573(3)	2427(2)	8856(2)	10(1)
O(1)	9195(3)	1782(2)	5089(1)	15(1)
O(2)	8677(2)	4842(2)	6188(1)	13(1)
O(3)	11344(2)	2563(2)	7358(1)	14(1)
O(4)	6691(3)	4116(2)	8893(1)	16(1)
O(5)	6391(3)	1532(2)	9796(1)	21(1)

Table 5.3 - Complete bond lengths (\AA) for arsonoacetic acid

As(1)-O(2)	1.6461(12)	C(1)-H(12)	0.99
As(1)-O(1)	1.7013(13)	C(2)-O(5)	1.210(2)
As(1)-O(3)	1.7072(13)	C(2)-O(4)	1.3117(19)
As(1)-C(1)	1.9185(17)	O(1)-H(1)	0.57(9)
C(1)-C(2)	1.509(2)	O(3)-H(2)	0.63(6)
C(1)-H(11)	0.99	O(4)-H(3)	0.92(3)

Table 5.4 - Complete bond angles ($^\circ$) for arsonoacetic acid

O(2)-As(1)-O(1)	105.04(6)	C(2)-C(1)-H(12)	109.3
O(2)-As(1)-O(3)	106.93(7)	As(1)-C(1)-H(12)	109.3
O(1)-As(1)-O(3)	109.24(7)	H(11)-C(1)-H(12)	107.9
O(2)-As(1)-C(1)	117.38(7)	O(5)-C(2)-O(4)	123.61(16)
O(1)-As(1)-C(1)	110.25(7)	O(5)-C(2)-C(1)	123.54(15)
O(3)-As(1)-C(1)	107.77(7)	O(4)-C(2)-C(1)	112.84(15)
C(2)-C(1)-As(1)	111.76(11)	As(1)-O(1)-H(1)	125(6)
C(2)-C(1)-H(11)	109.3	As(1)-O(3)-H(2)	130(5)
As(1)-C(1)-H(11)	109.3	C(2)-O(4)-H(3)	108(3)

**Table 5.5 - Anisotropic displacement parameters ($\text{\AA}^2 \times 10^3$) for arsonoacetic acid. The anisotropic displacement factor exponent takes the form:
 $-2\pi^2[h^2a^{*2}U^{11} + \dots + 2hka^*b^*U^{12}]$**

	U^{11}	U^{22}	U^{33}	U^{23}	U^{13}	U^{12}
As(1)	13(1)	6(1)	4(1)	0(1)	0(1)	0(1)
C(1)	14(1)	10(1)	8(1)	-1(1)	0(1)	-2(1)
C(2)	11(1)	10(1)	9(1)	0(1)	1(1)	-1(1)
O(1)	27(1)	11(1)	8(1)	-3(1)	3(1)	0(1)
O(2)	26(1)	5(1)	8(1)	1(1)	-2(1)	0(1)
O(3)	14(1)	16(1)	12(1)	6(1)	-3(1)	-3(1)
O(4)	30(1)	9(1)	8(1)	0(1)	2(1)	1(1)
O(5)	41(1)	12(1)	10(1)	2(1)	5(1)	-3(1)

Table 5.6 - Hydrogen coordinates ($\times 10^4$) and isotropic displacement parameters ($\text{\AA}^2 \times 10^3$) for arsonoacetic acid

	x	y	z	U(eq)
H(11)	5229	1922	7089	13
H(12)	6911	461	7548	13
H(1)	9690(130)	1170(120)	5000(50)	160(30)
H(2)	11640(80)	2000(90)	7750(60)	120(20)
H(3)	6480(50)	4450(50)	9720(30)	45(10)

Table 5.7 - Torsion angles ($^\circ$) for arsonoacetic acid

O(2)-As(1)-C(1)-C(2)	-66.78(13)
O(1)-As(1)-C(1)-C(2)	173.05(11)
O(3)-As(1)-C(1)-C(2)	53.90(13)
As(1)-C(1)-C(2)-O(5)	-134.78(16)
As(1)-C(1)-C(2)-O(4)	45.96(18)

Table 5.8 - Hydrogen bonds for arsonoacetic acid (Å and °)

D-H...A	d(D-H)	d(H...A)	d(D...A)	<(DHA)
O(2)-H(2)···O(5) ⁱ	0.84	1.82	2.612(2)	156.1
O(1)-H(1)···O(3) ⁱⁱ	0.84	1.79	2.6050(18)	162.8
O(4)-H(4)···O(3) ⁱⁱⁱ	0.84	1.71	2.544(2)	170.6

Symmetry transformations used to generate equivalent atoms:

(i): $-x+3/2, -y, z-1/2$

(ii): $-x+2, y-1/2, -z+3/2$

(iii): $-x+3/2, -y+1, z+1/2$

5.2 Cyclohexaarsenoacetic acid – $\text{As}_6(\text{CH}_2\text{COOH})_6 \cdot 6\text{C}_5\text{NH}_5$

Table 5.9 - Complete crystal data and structure refinement for arsenoacetic acid

Empirical formula	$\text{C}_{42}\text{H}_{48}\text{As}_6\text{N}_6\text{O}_{12}$
Formula weight	1278.38
Temperature	90(2) K
Wavelength	0.71073 Å
Crystal system	Triclinic
Space group	P-1
Unit cell dimensions	$a = 10.14560(1) \text{ Å}$ $\alpha = 113.9480(1)^\circ$ $b = 11.62330(1) \text{ Å}$ $\beta = 92.3780(1)^\circ$ $c = 12.4298(2) \text{ Å}$ $\gamma = 106.7160(1)^\circ$
Volume	$1261.85(3) \text{ Å}^3$
Z	1
Density (calculated)	1.682 Mg/m^3
Absorption coefficient	3.989 mm^{-1}
F(000)	636
Crystal size	$0.29 \times 0.20 \times 0.17 \text{ mm}^3$
Theta range for data collection	1.82 to 28.10°
Index ranges	$-13 \leq h \leq 13$, $-15 \leq k \leq 15$, $-16 \leq l \leq 16$
Reflections collected	37809
Independent reflections	6128 [R(int) = 0.0384]
Completeness to theta = 28.10°	99.30 %
Max. and min. transmission	0.5504 and 0.3908
Refinement method	Full-matrix least-squares on F^2
Data / restraints / parameters	6128 / 0 / 310
Goodness-of-fit on F^2	1.035
Final R indices [$I > 2\sigma(I)$]	R1 = 0.0221, wR2 = 0.0441
R indices (all data)	R1 = 0.0322, wR2 = 0.0466
Largest diff. peak and hole	0.449 and -0.304 e Å^{-3}

Table 5.10 - Atomic coordinates ($\times 10^4$) and equivalent isotropic displacement parameters ($\text{\AA}^2 \times 10^3$) for arsenoacetic acid. U(eq) is defined as one third of the trace of the orthogonalized U^{ij} tensor

	x	y	z	U(eq)
As(1)	7926(1)	3810(1)	4116(1)	13(1)
As(2)	8634(1)	5759(1)	6080(1)	13(1)
As(3)	10345(1)	4886(1)	6652(1)	13(1)
O(11)	6467(1)	6360(1)	4657(1)	22(1)
O(12)	6797(2)	5628(1)	2750(1)	20(1)
O(21)	6292(1)	2708(1)	5930(1)	22(1)
O(22)	7529(2)	3848(1)	7801(1)	22(1)
O(31)	10323(2)	8141(1)	8806(1)	24(1)
O(32)	12530(2)	8160(1)	8640(1)	23(1)
N(4)	2690(2)	-1439(2)	2383(1)	20(1)
N(5)	7816(2)	-1863(2)	3265(2)	21(1)
N(6)	6818(2)	9277(2)	10781(2)	23(1)
C(11)	6204(2)	4064(2)	3549(2)	16(1)
C(12)	6484(2)	5465(2)	3714(2)	16(1)
C(21)	7065(2)	5093(2)	6826(2)	18(1)
C(22)	6905(2)	3770(2)	6794(2)	17(1)
C(31)	10864(2)	6150(2)	8394(2)	19(1)
C(32)	11190(2)	7580(2)	8640(2)	20(1)
C(41)	3591(2)	-350(2)	3288(2)	21(1)
C(42)	3809(2)	932(2)	3419(2)	22(1)
C(43)	3066(2)	1103(2)	2572(2)	23(1)
C(44)	2131(2)	-8(2)	1625(2)	22(1)
C(45)	1981(2)	-1251(2)	1572(2)	22(1)
C(51)	9179(2)	-1318(2)	3308(2)	24(1)
C(52)	9812(2)	33(2)	3661(2)	27(1)
C(53)	9003(2)	845(2)	3977(2)	27(1)
C(54)	7599(2)	299(2)	3947(2)	28(1)
C(55)	7044(2)	-1062(2)	3592(2)	26(1)
C(61)	5478(2)	8496(2)	10483(2)	32(1)

C(62)	5080(3)	7123(2)	10005(2)	37(1)
C(63)	6090(3)	6533(2)	9831(2)	33(1)
C(64)	7477(2)	7327(2)	10141(2)	30(1)
C(65)	7794(2)	8694(2)	10610(2)	25(1)

Table 5.11 - Complete bond lengths (Å) for arsenoacetic acid

As(1)-C(11)	1.9994(19)	C(31)-H(31A)	0.99
As(1)-As(2)	2.4566(3)	C(31)-H(31B)	0.99
As(1)-As(3) ⁱ	2.4628(3)	C(41)-C(42)	1.381(3)
As(2)-C(21)	1.9969(18)	C(41)-H(41)	0.95
As(2)-As(3)	2.4589(3)	C(42)-C(43)	1.381(3)
As(3)-C(31)	2.0006(18)	C(42)-H(42)	0.95
As(3)-As(1) ⁱ	2.4628(3)	C(43)-C(44)	1.386(3)
O(11)-C(12)	1.216(2)	C(43)-H(43)	0.95
O(12)-C(12)	1.324(2)	C(44)-C(45)	1.382(3)
O(12)-H(1)	0.85(3)	C(44)-H(44)	0.95
O(21)-C(22)	1.220(2)	C(45)-H(45)	0.95
O(22)-C(22)	1.336(2)	C(51)-C(52)	1.381(3)
O(22)-H(2)	0.82(3)	C(51)-H(51)	0.95
O(31)-C(32)	1.215(2)	C(52)-C(53)	1.375(3)
O(32)-C(32)	1.332(2)	C(52)-H(52)	0.95
O(32)-H(3)	0.89(3)	C(53)-C(54)	1.375(3)
N(4)-C(45)	1.338(3)	C(53)-H(53)	0.95
N(4)-C(41)	1.341(2)	C(54)-C(55)	1.384(3)
N(5)-C(51)	1.334(3)	C(54)-H(54)	0.95
N(5)-C(55)	1.334(3)	C(55)-H(55)	0.95
N(6)-C(65)	1.331(3)	C(61)-C(62)	1.380(3)
N(6)-C(61)	1.335(3)	C(61)-H(61)	0.95
C(11)-C(12)	1.494(3)	C(62)-C(63)	1.367(3)
C(11)-H(11A)	0.99	C(62)-H(62)	0.95
C(11)-H(11B)	0.99	C(63)-C(64)	1.378(3)
C(21)-C(22)	1.483(3)	C(63)-H(63)	0.95

C(21)-H(21A)	0.99	C(64)-C(65)	1.381(3)
C(21)-H(21B)	0.99	C(64)-H(64)	0.95
C(31)-C(32)	1.493(3)	C(65)-H(65)	0.95

Symmetry transformations used to generate equivalent atoms:

(i): -x+2, -y+1, -z+1

Table 5.12 - Complete bond angles (°) for arsenoacetic acid

C(11)-As(1)-As(2)	97.92(5)	C(42)-C(41)-H(41)	118.3
C(11)-As(1)-As(3) ⁱ	99.38(5)	C(43)-C(42)-C(41)	118.37(18)
As(2)-As(1)-As(3) ⁱ	88.753(8)	C(43)-C(42)-H(42)	120.8
C(21)-As(2)-As(1)	97.19(6)	C(41)-C(42)-H(42)	120.8
C(21)-As(2)-As(3)	99.52(6)	C(42)-C(43)-C(44)	119.37(19)
As(1)-As(2)-As(3)	89.228(9)	C(42)-C(43)-H(43)	120.3
C(31)-As(3)-As(2)	97.93(6)	C(44)-C(43)-H(43)	120.3
C(31)-As(3)-As(1) ⁱ	99.19(6)	C(45)-C(44)-C(43)	118.05(19)
As(2)-As(3)-As(1) ⁱ	87.856(9)	C(45)-C(44)-H(44)	121
C(12)-O(12)-H(1)	111.9(18)	C(43)-C(44)-H(44)	121
C(22)-O(22)-H(2)	110.0(17)	N(4)-C(45)-C(44)	123.59(18)
C(32)-O(32)-H(3)	112.1(19)	N(4)-C(45)-H(45)	118.2
C(45)-N(4)-C(41)	117.24(17)	C(44)-C(45)-H(45)	118.2
C(51)-N(5)-C(55)	118.37(17)	N(5)-C(51)-C(52)	122.5(2)
C(65)-N(6)-C(61)	118.06(19)	N(5)-C(51)-H(51)	118.7
C(12)-C(11)-As(1)	111.55(12)	C(52)-C(51)-H(51)	118.7
C(12)-C(11)-H(11A)	109.3	C(53)-C(52)-C(51)	118.6(2)
As(1)-C(11)-H(11A)	109.3	C(53)-C(52)-H(52)	120.7
C(12)-C(11)-H(11B)	109.3	C(51)-C(52)-H(52)	120.7
As(1)-C(11)-H(11B)	109.3	C(54)-C(53)-C(52)	119.42(19)
H(11A)-C(11)-H(11B)	108	C(54)-C(53)-H(53)	120.3
O(11)-C(12)-O(12)	124.27(17)	C(52)-C(53)-H(53)	120.3
O(11)-C(12)-C(11)	122.59(17)	C(53)-C(54)-C(55)	118.5(2)
O(12)-C(12)-C(11)	113.10(16)	C(53)-C(54)-H(54)	120.7
C(22)-C(21)-As(2)	114.77(13)	C(55)-C(54)-H(54)	120.7

C(22)-C(21)-H(21A)	108.6	N(5)-C(55)-C(54)	122.5(2)
As(2)-C(21)-H(21A)	108.6	N(5)-C(55)-H(55)	118.7
C(22)-C(21)-H(21B)	108.6	C(54)-C(55)-H(55)	118.7
As(2)-C(21)-H(21B)	108.6	N(6)-C(61)-C(62)	122.5(2)
H(21A)-C(21)-H(21B)	107.6	N(6)-C(61)-H(61)	118.8
O(21)-C(22)-O(22)	122.75(18)	C(62)-C(61)-H(61)	118.8
O(21)-C(22)-C(21)	123.96(18)	C(63)-C(62)-C(61)	119.1(2)
O(22)-C(22)-C(21)	113.27(16)	C(63)-C(62)-H(62)	120.5
C(32)-C(31)-As(3)	113.86(13)	C(61)-C(62)-H(62)	120.5
C(32)-C(31)-H(31A)	108.8	C(62)-C(63)-C(64)	119.1(2)
As(3)-C(31)-H(31A)	108.8	C(62)-C(63)-H(63)	120.5
C(32)-C(31)-H(31B)	108.8	C(64)-C(63)-H(63)	120.5
As(3)-C(31)-H(31B)	108.8	C(63)-C(64)-C(65)	118.5(2)
H(31A)-C(31)-H(31B)	107.7	C(63)-C(64)-H(64)	120.7
O(31)-C(32)-O(32)	124.10(18)	C(65)-C(64)-H(64)	120.7
O(31)-C(32)-C(31)	123.54(18)	N(6)-C(65)-C(64)	122.8(2)
O(32)-C(32)-C(31)	112.35(18)	N(6)-C(65)-H(65)	118.6
N(4)-C(41)-C(42)	123.38(19)	C(64)-C(65)-H(65)	118.6
N(4)-C(41)-H(41)	118.3		

Symmetry transformations used to generate equivalent atoms:

(i): -x+2, -y+1, -z+1

Table 5.13 - Anisotropic displacement parameters ($\text{\AA}^2 \times 10^3$) for arsenoacetic acid. The anisotropic displacement factor exponent takes the form:
 $-2\pi^2[h^2a^{*2}U^{11} + \dots + 2hka^*b^*U^{12}]$

	U^{11}	U^{22}	U^{33}	U^{23}	U^{13}	U^{12}
As(1)	12(1)	11(1)	16(1)	5(1)	2(1)	4(1)
As(2)	12(1)	11(1)	16(1)	5(1)	2(1)	4(1)
As(3)	12(1)	12(1)	15(1)	5(1)	2(1)	3(1)
O(11)	23(1)	18(1)	24(1)	7(1)	7(1)	10(1)
O(12)	25(1)	16(1)	21(1)	10(1)	4(1)	6(1)
O(21)	20(1)	18(1)	23(1)	7(1)	1(1)	3(1)

O(22)	29(1)	16(1)	19(1)	8(1)	1(1)	4(1)
O(31)	22(1)	21(1)	24(1)	4(1)	4(1)	8(1)
O(32)	17(1)	19(1)	26(1)	6(1)	4(1)	2(1)
N(4)	22(1)	16(1)	18(1)	6(1)	6(1)	4(1)
N(5)	27(1)	19(1)	22(1)	11(1)	8(1)	8(1)
N(6)	21(1)	23(1)	21(1)	7(1)	3(1)	3(1)
C(11)	11(1)	17(1)	20(1)	8(1)	1(1)	4(1)
C(12)	8(1)	19(1)	22(1)	9(1)	1(1)	5(1)
C(21)	14(1)	20(1)	22(1)	10(1)	7(1)	7(1)
C(22)	12(1)	20(1)	20(1)	8(1)	7(1)	4(1)
C(31)	20(1)	21(1)	13(1)	7(1)	2(1)	4(1)
C(32)	20(1)	21(1)	11(1)	3(1)	1(1)	3(1)
C(41)	18(1)	22(1)	21(1)	9(1)	1(1)	7(1)
C(42)	19(1)	17(1)	24(1)	5(1)	1(1)	3(1)
C(43)	22(1)	18(1)	29(1)	12(1)	7(1)	6(1)
C(44)	21(1)	26(1)	20(1)	13(1)	3(1)	6(1)
C(45)	22(1)	22(1)	14(1)	6(1)	2(1)	1(1)
C(51)	25(1)	27(1)	24(1)	12(1)	9(1)	14(1)
C(52)	22(1)	28(1)	28(1)	12(1)	9(1)	4(1)
C(53)	33(1)	17(1)	29(1)	12(1)	7(1)	4(1)
C(54)	31(1)	22(1)	38(1)	14(1)	13(1)	15(1)
C(55)	22(1)	25(1)	35(1)	16(1)	11(1)	9(1)
C(61)	19(1)	33(1)	42(1)	17(1)	6(1)	5(1)
C(62)	23(1)	32(1)	43(1)	13(1)	1(1)	-5(1)
C(63)	42(2)	22(1)	29(1)	10(1)	10(1)	3(1)
C(64)	33(1)	34(1)	30(1)	17(1)	14(1)	16(1)
C(65)	18(1)	30(1)	23(1)	12(1)	2(1)	2(1)

Table 5.14 – Hydrogen coordinates ($\times 10^4$) and isotropic displacement parameters ($\text{\AA}^2 \times 10^3$) for arsenoacetic acid

	x	y	z	U(eq)
H(1)	7120(30)	6450(30)	2900(20)	48(8)
H(2)	7450(30)	3100(30)	7730(20)	37(7)
H(3)	12710(30)	9010(30)	8770(20)	57(9)
H(11A)	5857	3443	2691	19
H(11B)	5465	3845	3999	19
H(21A)	7214	5752	7671	22
H(21B)	6181	5040	6411	22
H(31A)	10082	5905	8796	23
H(31B)	11690	6046	8747	23
H(41)	4106	-467	3869	25
H(42)	4455	1679	4076	27
H(43)	3194	1972	2638	27
H(44)	1608	83	1030	26
H(45)	1340	-2013	924	26
H(51)	9735	-1881	3087	29
H(52)	10786	393	3685	32
H(53)	9411	1776	4212	32
H(54)	7023	843	4166	34
H(55)	6077	-1442	3582	31
H(61)	4773	8902	10604	38
H(62)	4118	6595	9799	45
H(63)	5840	5589	9502	40
H(64)	8199	6942	10033	36
H(65)	8750	9242	10821	30

Table 5.15 - Torsion angles (°) for arsenoacetic acid

C(11)-As(1)-As(2)-C(21)	69.07(8)
As(3) ⁱ -As(1)-As(2)-C(21)	168.37(6)
C(11)-As(1)-As(2)-As(3)	168.57(5)
As(3) ⁱ -As(1)-As(2)-As(3)	-92.128(8)
C(21)-As(2)-As(3)-C(31)	-72.63(8)
As(1)-As(2)-As(3)-C(31)	-169.79(6)
C(21)-As(2)-As(3)-As(1) ⁱ	-171.62(6)
As(1)-As(2)-As(3)-As(1) ⁱ	91.219(8)
As(2)-As(1)-C(11)-C(12)	48.96(13)
As(3) ⁱ -As(1)-C(11)-C(12)	-41.08(14)
As(1)-C(11)-C(12)-O(11)	-83.9(2)
As(1)-C(11)-C(12)-O(12)	93.87(16)
As(1)-As(2)-C(21)-C(22)	54.90(14)
As(3)-As(2)-C(21)-C(22)	-35.53(14)
As(2)-C(21)-C(22)-O(21)	-82.4(2)
As(2)-C(21)-C(22)-O(22)	96.22(17)
As(2)-As(3)-C(31)-C(32)	-48.18(15)
As(1) ⁱ -As(3)-C(31)-C(32)	40.92(15)
As(3)-C(31)-C(32)-O(31)	91.5(2)
As(3)-C(31)-C(32)-O(32)	-87.56(17)
C(45)-N(4)-C(41)-C(42)	0.3(3)
N(4)-C(41)-C(42)-C(43)	-0.3(3)
C(41)-C(42)-C(43)-C(44)	0.1(3)
C(42)-C(43)-C(44)-C(45)	0.1(3)
C(41)-N(4)-C(45)-C(44)	-0.1(3)
C(43)-C(44)-C(45)-N(4)	-0.1(3)
C(55)-N(5)-C(51)-C(52)	-1.0(3)
N(5)-C(51)-C(52)-C(53)	-0.2(3)
C(51)-C(52)-C(53)-C(54)	0.8(3)
C(52)-C(53)-C(54)-C(55)	-0.4(3)
C(51)-N(5)-C(55)-C(54)	1.5(3)

C(53)-C(54)-C(55)-N(5)	-0.8(3)
C(65)-N(6)-C(61)-C(62)	-0.3(3)
N(6)-C(61)-C(62)-C(63)	0.2(4)
C(61)-C(62)-C(63)-C(64)	0.1(4)
C(62)-C(63)-C(64)-C(65)	-0.4(3)
C(61)-N(6)-C(65)-C(64)	0.0(3)
C(63)-C(64)-C(65)-N(6)	0.3(3)

Symmetry transformations used to generate equivalent atoms:

(i): $-x+2, -y+1, -z+1$

Table 5.16 - Hydrogen bonds for arsenoacetic acid (Å and °)

D-H...A	d(D-H)	d(H...A)	d(D...A)	<(DHA)
O(12)-H(1)...N(5) ⁱⁱ	0.85(3)	1.74(3)	2.585(2)	178(3)
O(22)-H(2)...N(4) ⁱⁱⁱ	0.82(3)	1.84(3)	2.658(2)	178(3)
O(32)-H(3)...N(6) ^{iv}	0.89(3)	1.74(3)	2.630(2)	172(3)

Symmetry transformations used to generate equivalent atoms:

(ii): $x, y+1, z$

(iii): $-x+1, -y, -z+1$

(iv): $-x+2, -y+2, -z+2$

5.3 β -Monoclinic S_8 (β - S_8)

Table 5.17 - Crystal data and structure refinement for β - S_8

Empirical formula	S_8
Formula weight	256.48
Temperature	90(2) K
Wavelength	0.71073 Å
Crystal system	$P2_1$
Space group	Monoclinic
Unit cell dimensions	$a = 10.67360(10)$ Å $b = 10.70140(10)$ Å $\beta = 95.7110(10)^\circ$ $c = 10.81390(10)$ Å
Volume	$1229.06(2)$ Å ³
Z	6
Density (calculated)	2.079 Mg/m ³
Absorption coefficient	2.078 mm ⁻¹
F(000)	768
Crystal size	$0.30 \times 0.30 \times 0.27$ mm ³
Theta range for data collection	1.89 to 27.86°
Index ranges	$-13 \leq h \leq 14$, $-14 \leq k \leq 12$, $-13 \leq l \leq 14$
Reflections collected	15373
Independent reflections	5429 [R(int) = 0.0196]
Completeness to theta = 27.86°	99.4 %
Max. and min. transmission	0.6039 and 0.5745
Refinement method	Full-matrix least-squares on F^2
Data / restraints / parameters	5429 / 1 / 217
Goodness-of-fit on F^2	1.090
Final R indices [$I > 2\sigma(I)$]	$R1 = 0.0208$, $wR2 = 0.0511$
R indices (all data)	$R1 = 0.0213$, $wR2 = 0.0514$
Largest diff. peak and hole	0.357 and -0.270 e Å ⁻³

Table 5.18 - Atomic coordinates ($\times 10^4$) and equivalent isotropic displacement parameters ($\text{\AA}^2 \times 10^3$) for β -S₈. U(eq) is defined as one third of the trace of the orthogonalized U^{ij} tensor

	x	y	z	U(eq)
S(11)	452(1)	1002(1)	6751(1)	19(1)
S(12)	2187(1)	986(1)	7761(1)	19(1)
S(13)	2418(1)	2718(1)	8574(1)	21(1)
S(14)	3540(1)	3761(1)	7533(1)	21(1)
S(15)	2377(1)	4865(1)	6361(1)	21(1)
S(16)	2151(1)	4000(1)	4658(1)	17(1)
S(17)	429(1)	3118(1)	4508(1)	17(1)
S(18)	723(1)	1263(1)	4915(1)	17(1)
S(21)	7387(1)	2677(1)	6181(1)	21(1)
S(22)	7094(1)	3535(1)	4480(1)	17(1)
S(23)	5390(1)	4452(1)	4398(1)	17(1)
S(24)	5726(1)	6304(1)	4795(1)	17(1)
S(25)	5533(1)	6562(1)	6646(1)	19(1)
S(26)	7304(1)	6564(1)	7593(1)	18(1)
S(27)	7537(1)	4833(1)	8388(1)	22(1)
S(28)	8606(1)	3766(1)	7310(1)	21(1)
S(31)	8257(1)	-25(1)	8402(1)	21(1)
S(32)	6484(1)	-476(1)	8824(1)	19(1)
S(33)	5464(1)	1152(1)	8758(1)	24(1)
S(34)	5444(1)	1749(1)	10558(1)	24(1)
S(35)	6737(1)	3154(1)	10885(1)	24(1)
S(36)	8371(1)	2424(1)	11763(1)	24(1)
S(37)	9571(1)	2048(1)	10439(1)	25(1)
S(38)	9419(1)	175(1)	10021(1)	24(1)

Table 5.19 - Bond lengths (Å) for β -S₈

S(11)-S(18)	2.0530(10)	S(24)-S(25)	2.0506(10)
S(11)-S(12)	2.0547(10)	S(25)-S(26)	2.0587(10)
S(12)-S(13)	2.0557(11)	S(26)-S(27)	2.0465(11)
S(13)-S(14)	2.0538(11)	S(27)-S(28)	2.0560(11)
S(14)-S(15)	2.0563(11)	S(31)-S(32)	2.0478(10)
S(15)-S(16)	2.0541(10)	S(31)-S(38)	2.0533(10)
S(16)-S(17)	2.0581(10)	S(32)-S(33)	2.0515(11)
S(17)-S(18)	2.0508(11)	S(33)-S(34)	2.0508(11)
S(21)-S(22)	2.0520(10)	S(34)-S(35)	2.0476(12)
S(21)-S(28)	2.0552(10)	S(35)-S(36)	2.0560(11)
S(22)-S(23)	2.0607(10)	S(36)-S(37)	2.0536(11)
S(23)-S(24)	2.0521(11)	S(37)-S(38)	2.0578(11)

Table 5.20 - Bond angles (°) for β -S₈

S(18)-S(11)-S(12)	108.00(4)	S(24)-S(25)-S(26)	108.01(4)
S(11)-S(12)-S(13)	106.48(5)	S(27)-S(26)-S(25)	105.99(5)
S(14)-S(13)-S(12)	107.91(4)	S(26)-S(27)-S(28)	108.40(4)
S(13)-S(14)-S(15)	107.51(4)	S(21)-S(28)-S(27)	107.33(4)
S(16)-S(15)-S(14)	107.66(4)	S(32)-S(31)-S(38)	109.12(4)
S(15)-S(16)-S(17)	107.56(4)	S(31)-S(32)-S(33)	106.93(5)
S(18)-S(17)-S(16)	108.09(4)	S(34)-S(33)-S(32)	106.68(5)
S(17)-S(18)-S(11)	107.83(4)	S(35)-S(34)-S(33)	108.81(5)
S(22)-S(21)-S(28)	108.04(5)	S(34)-S(35)-S(36)	109.10(5)
S(21)-S(22)-S(23)	107.88(4)	S(37)-S(36)-S(35)	108.18(5)
S(24)-S(23)-S(22)	108.42(4)	S(36)-S(37)-S(38)	107.63(5)
S(25)-S(24)-S(23)	107.58(4)	S(31)-S(38)-S(37)	108.46(5)

Table 5.21 - Anisotropic displacement parameters ($\text{\AA}^2 \times 10^3$) for β -S₈. The anisotropic displacement factor exponent takes the form: $-2\pi^2 [h^2 a^{*2} U^{11} + \dots + 2 h k a^* b^* U^{12}]$

	U^{11}	U^{22}	U^{33}	U^{23}	U^{13}	U^{12}
S(11)	17(1)	19(1)	23(1)	1(1)	5(1)	-4(1)
S(12)	22(1)	15(1)	20(1)	1(1)	1(1)	1(1)
S(13)	28(1)	21(1)	15(1)	-4(1)	1(1)	1(1)
S(14)	20(1)	20(1)	23(1)	-2(1)	-5(1)	-3(1)
S(15)	25(1)	12(1)	24(1)	-3(1)	-2(1)	-1(1)
S(16)	16(1)	16(1)	18(1)	2(1)	2(1)	-1(1)
S(17)	14(1)	17(1)	21(1)	0(1)	-2(1)	1(1)
S(18)	19(1)	14(1)	19(1)	-3(1)	1(1)	-2(1)
S(21)	24(1)	14(1)	24(1)	3(1)	-6(1)	-2(1)
S(22)	16(1)	16(1)	18(1)	-2(1)	1(1)	2(1)
S(23)	13(1)	17(1)	19(1)	0(1)	-2(1)	-1(1)
S(24)	20(1)	15(1)	17(1)	3(1)	2(1)	2(1)
S(25)	18(1)	22(1)	19(1)	-2(1)	3(1)	5(1)
S(26)	20(1)	18(1)	18(1)	-3(1)	2(1)	-1(1)
S(27)	26(1)	26(1)	14(1)	4(1)	-1(1)	-3(1)
S(28)	20(1)	18(1)	24(1)	1(1)	-7(1)	3(1)
S(31)	19(1)	26(1)	20(1)	-6(1)	6(1)	-2(1)
S(32)	16(1)	18(1)	22(1)	-2(1)	1(1)	-2(1)
S(33)	21(1)	28(1)	23(1)	-5(1)	-4(1)	6(1)
S(34)	22(1)	28(1)	25(1)	-4(1)	7(1)	1(1)
S(35)	33(1)	16(1)	22(1)	-1(1)	-1(1)	4(1)
S(36)	31(1)	23(1)	16(1)	-2(1)	-4(1)	-1(1)
S(37)	23(1)	23(1)	28(1)	-2(1)	0(1)	-9(1)
S(38)	17(1)	22(1)	31(1)	-3(1)	-4(1)	1(1)

Table 5.22 - Torsion angles (°) for β -S₈

S(18)-S(11)-S(12)-S(13)	101.42(5)
S(11)-S(12)-S(13)-S(14)	-100.14(5)
S(12)-S(13)-S(14)-S(15)	97.75(5)
S(13)-S(14)-S(15)-S(16)	-98.38(5)
S(14)-S(15)-S(16)-S(17)	101.01(5)
S(15)-S(16)-S(17)-S(18)	-99.41(5)
S(16)-S(17)-S(18)-S(11)	96.46(5)
S(12)-S(11)-S(18)-S(17)	-98.78(5)
S(28)-S(21)-S(22)-S(23)	-100.45(5)
S(21)-S(22)-S(23)-S(24)	98.89(5)
S(22)-S(23)-S(24)-S(25)	-96.37(5)
S(23)-S(24)-S(25)-S(26)	99.16(5)
S(24)-S(25)-S(26)-S(27)	-101.56(5)
S(25)-S(26)-S(27)-S(28)	100.37(5)
S(22)-S(21)-S(28)-S(27)	97.84(5)
S(26)-S(27)-S(28)-S(21)	-98.02(5)
S(38)-S(31)-S(32)-S(33)	97.61(5)
S(31)-S(32)-S(33)-S(34)	-99.53(5)
S(32)-S(33)-S(34)-S(35)	101.34(5)
S(33)-S(34)-S(35)-S(36)	-98.08(5)
S(34)-S(35)-S(36)-S(37)	95.76(5)
S(35)-S(36)-S(37)-S(38)	-98.21(5)
S(32)-S(31)-S(38)-S(37)	-98.43(5)
S(36)-S(37)-S(38)-S(31)	99.75(5)

6. References

1. Cullen, W. R., *Is Arsenic an Aphrodisiac? The Sociochemistry of an Element*. RSC Publishing: Cambridge, 2008.
2. Antman, K. H., Introduction: The history of arsenic trioxide in cancer therapy. *Oncologist* 2001, **6**, 1-2.
3. Waxman, S.; Anderson, K. C., History of the development of arsenic derivatives in cancer therapy. *Oncologist* 2001, **6**, 3-10.
4. Gielen, M.; Tiekink, E. R. T., *Metallotherapeutic Drugs and Metal-Based Diagnostic Agents: The Use of Metals in Medicine*. Wiley: Chichester, England, 2005.
5. Emsley, J., *The Elements of Murder*. Oxford University Press: Oxford, 2006.
6. Nriagu, J. O., *Arsenic in the Environment, Part I: Cycling and Characterization*. Wiley: New York, 1994.
7. Emsley, J., *Nature's Building Blocks: An A-Z Guide to the Elements*. Oxford University Press: New York, 2002.
8. Nriagu, J. O., *Arsenic in the Environment, Part II: Human Health and Ecosystem Effects*. Wiley: New York, 1994.
9. Jolliffe, D. M., A history of the use of arsenicals in man. *J. R. Soc. Med.* 1993, **86**, 287-289.
10. Przgodna, G.; Feldmann, J.; Cullen, W. R., The arsenic eaters of Styria: a different picture of people who were chronically exposed to arsenic. *Appl. Organomet. Chem.* 2001, **15**, 457-462.
11. Cyranoski, D., Arsenic patent keeps drug for rare cancer out of reach of many. *Nat. Med.* 2007, **13**, 1005.

12. Soignet, S. L.; Maslak, P.; Wang, Z.-G.; Jhanwar, S., Complete remission after treatment of acute promyelocytic leukemia with arsenic trioxide. *N. Engl. J. Med.* 1998, **339**, 1341-1349.
13. Chen, G. Q.; Zhu, J.; Shi, X. G.; Ni, J. H.; Zhong, H. J.; Si, G. Y.; Jin, X. L.; Tang, W.; Li, X. S.; Xong, S. M.; Shen, Z. X.; Sun, G. L.; Ma, J.; Zhang, P.; Zhang, T. D.; Gazin, C.; Naoe, T.; Chen, S. J.; Wang, Z. Y.; Chen, Z., In vitro studies on cellular and molecular mechanisms of arsenic trioxide (As_2O_3) in the treatment of acute promyelocytic leukemia: As_2O_3 induces NB_4 cell apoptosis with downregulation of Bcl-2 expression and modulation of PML-RAR α /PML proteins. *Blood* 1996, **88**, 1052-1061.
14. Dilda, P. J.; Hogg, P. J., Arsenical-based cancer drugs. *Cancer Treat. Rev.* 2007, **33**, 542-564.
15. Wattell Jr. *et al.* Process for producing arsenic trioxide formulations and methods for treating cancer using arsenic trioxide or melarsoprol. US Patent 6770304 B2, 2004.
16. Douer, D.; Hu, W.; Giralt, S.; Lill, M.; DiPersio, J., Arsenic trioxide (Trisenox[®]) therapy for acute promyelocytic leukemia in the setting of hematopoietic stem cell transplantation. *Oncologist* 2003, **8**, 132-140.
17. Lloyd, N. C.; Morgan, H. W.; Nicholson, B. K.; Ronimus, R. S., The composition of Ehrlich's salvarsan: resolution of a century-old debate. *Angew. Chem., Int. Ed.* 2005, **44**, 941-944.
18. Dhubhghaill, O. M. N.; Sadler, P. J., The structure and reactivity of arsenic compounds: biological activity and drug design. *Struct. Bonding (Berlin)* 1991, **78**, 129-190.
19. Lykknes, A.; Kvittingen, L., Arsenic: not so evil after all? *J. Chem. Educ.* 2003, **50**, 497-500.
20. Twamley, B.; Sofield, C. D.; Olmstead, M.; Power, P., Homologous series of heavier element dipnictenes 2,6-Ar₂H₃C₆E=EC₆H₃-2,6-Ar₂ (E = P, As,

- Sb, Bi; Ar = Mes = C₆H₂-2,4,6-Me₃; or Trip = C₆H₂-2,4,6-ⁱPr₃) stabilized by *m*-terphenyl ligands. *J. Am. Chem. Soc.* 1999, **121**, 3357-5567.
21. Ratnaïke, R., Acute and chronic arsenic toxicity. *Postgrad. Med. J.* 2003, **79**, 391-398.
 22. Isbister, G. K.; Dawson, A. H.; Whyte, I. M., Arsenic trioxide poisoning: a description of two acute overdoses. *Hum. Exp. Toxicol.* 2004, **23**, 359-364.
 23. Fowler, B. A., *Biological and Environmental Effects of Arsenic*. Elsevier: New York, 1983.
 24. Hughes, M. F., Arsenic toxicity and potential mechanisms of action. *Toxicol. Lett.* 2002, **133**, 1-16.
 25. Basu, P.; Ghosh, R. N.; Grove, L. E.; Klei, L.; Barchowsky, A., Angiogenic potential of 3-nitro-4hydroxy benzene arsonic acid (Roxarsone). *Environ. Health Perspect.* 2008, **116**, 520-523.
 26. Chapman, H. D.; Johnson, Z. B., Use of antibiotics and Roxasone in broiler chickens in the USA: analysis for the years 1995 to 2000. *Poult. Sci.* 2002, **81**, 356-364.
 27. Hingston, J. A.; Collins, C. D.; Murphy, R. J.; Lester, J. N., Leaching of chromated copper arsenate wood preservatives: a review. *Environ. Pollut.* 2001, **111**, 53-66.
 28. Cho, A., New superconductors propel Chinese physicists to forefront. *Science* 2008, **320**, 432-433.
 29. Doak, G. O.; Freedman, L. D., *Organometallic Compounds of Arsenic, Antimony, and Bismuth*. Wiley-Interscience: New York, 1970.
 30. Bart, H. German Patent 250264, 1910.

31. Palmer, C. S.; Adams, R., The reactions of the arsines. II. Condensation of aromatic primary arsines with aldehydes. *J. Am. Chem. Soc.* 1922, **44**, 1356-1382.
32. Meyer, G., Ueber einige anomale reaktionen. *Chem. Ber.* 1883, **16**, 1439-1443.
33. Cullen, W. R., Organoarsenic chemistry. *Adv. Organomet. Chem.* 1966, **4**, 145-242.
34. Rosenmund, K. W., Das am ring-kohlenstoff gebundene halogen und sein ersatz durch andere substituenten, III. Mitteilung die darstellung von arsin- und sulfonsäuren. *Chem. Ber.* 1921, **54**, 438-440.
35. Gupta, V. K.; Krannich, L. K.; Watkins, C. L., Synthesis of cyclic polyarsines. *Synth. React. Inorg. Met.-Org. Chem.* 1987, **17**, 501-506.
36. Smith, L. R.; Mills, J. L., Cyclopolyarsines. *J. Organomet. Chem.* 1975, **84**, 1-15.
37. Palmer, C. S., Aliphatic arseno compounds. I arseno-acetic acid and tetra-arseno-acetic acid. *J. Am. Chem. Soc.* 1923, **45**, 3023-3029.
38. O'Neil, M. J., *The Merck index: an encyclopedia of chemicals, drugs, and biologicals*. 13th ed.; Merck Research Laboratories: Whitehouse Station, N.J., 2001.
39. Wang, J.; Wang, Y. Preparation of arsonoacetic acid derivatives as anticancer agents. Chinese Patent 1337400, 2003.
40. Palmer, C. S., Arsono- and arsenoacetic acids. *Org. Synth.* 1925, **4**, 5-7.
41. Palmer, C. S. Aliphatic arseno compound. US Patent 1794119, 1931.
42. Bremmer, B. J.; Sonnabend, L. F. Process for impregnating wood and products thereof. US Patent 3519476, 1970.

43. Tarello, W.; Riccieri, N. Use of arsenic for preparing a medicament for the treatment of premenstrual syndrome. European Patent EP0911031, 2004.
44. Tarello, W., Chronic fatigue syndrome in horses: diagnosis and treatment of 4 cases. *Comp. Immunol. Microbiol. Infect. Dis.* 2001, **24**, 57-70.
45. Weber, L.; Dembeck, G.; Lönneke, P.; Stammeler, H.-G.; Neumann, B., η^1 -Ligation versus pnictogen-carbon double bond cleavage: the contrasting behavior of phospho- and arsaalkenes $[\text{Tp}^*(\text{CO})_2\text{M}\equiv\text{C}-\text{E}=\text{C}(\text{NMe}_2)_2]$ $[\text{E} = \text{P, As}; \text{M} = \text{Mo, W}; \text{Tp}^* = \text{HB}(3,5\text{-Me}_2\text{pz})_3]$ toward $[\text{Au}(\text{CO})\text{Cl}]$. *Organometallics* 2001, **20**, 2288-2293.
46. Mandel, N.; Donohue, J., The molecular and crystal structure of trifluoromethylarsenic tetramer $(\text{AsCF}_3)_4$. *Acta Cryst.* 1971, **B24**, 476-480.
47. Mundt, O.; Becker, G.; Wessely, H.-J.; Breunig, H. J.; Kischkel, H., Element-element-bindungen. I. Synthese und struktur des tetra(tert-butyl)tetrarsetans und des tetra(tert-butyl)tetrastibetans. *Z. Anorg. Allg. Chem.* 1982, **486**, 70-89.
48. Burns, J. H.; Waser, J., The crystal structure of arsenomethane. *J. Am. Chem. Soc.* 1957, **79**, 859-864.
49. Wells, R. L.; Kwag, C.-Y.; Purdy, A. P.; Mcphail, A. T.; Pitt, C. G., Preparation and chemistry of $\text{Me}_3\text{SiCH}_2\text{AsH}_2$; Preparation of $[\text{Me}_3\text{SiCH}_2(\text{H})\text{AsGaPh}_2]_3$, a trimeric mono(arsino)gallane containing a hydrogen bonded to arsenic. Isolation and X-ray crystal structure of $(\text{Me}_3\text{SiCH}_2\text{As})_5$. *Polyhedron* 1990, **9**, 319-327.
50. Rheingold, A. L.; Kekia, O. M.; Strong, J. B., Structural studies of cyclopentaarsines. Crystallographic characterization of *cyclo*(PhAs)₅ and *cyclo*(*p*-TolAs)₅. *Main Group Chem.* 1997, **2**, 31-35.

51. Hedberg, K.; Hughes, E. W.; Waser, J., The structure of arsenobenzene. *Acta Cryst.* 1961, **14**, 369-374.
52. Rheingold, A. L.; Sullivan, P. J., Crystal and molecular structure of hexaphenylcyclohexaarsine, c-(AsPh)₆. *Organometallics* 1983, **2**, 327-331.
53. Marx, M. B. L.; Pritzkow, H.; Keppler, B. K., Darstellung und struktur von hexa(4-methoxyphenyl)cyclohexaarsan. *Z. Anorg. Allg. Chem.* 1997, **623**, 75-78.
54. Gottlieb, H. E.; Kotlyar, V.; Nudelman, A., NMR chemical shifts of common laboratory solvents as trace impurities. *J. Org. Chem.* 1997, **62**, 7512-7515.
55. Rozovskaya, T. A.; Rechinsky, V. O.; Bibilashvili, R. S.; Karpeisky, M. Y.; Tarusova, N. B.; Khomutov, R. M.; Dixon, H. B. F., The mechanism of pyrophosphorolysis of RNA by RNA polymerase. *Biochem. J.* 1984, **224**, 645-650.
56. Sparkes, M. J.; Dixon, H. B. F., Preparation of substituted methylarsonic and arsonoacetic acids. *Microbiology* 2008, **141**, 726-727.
57. Blessing, R. H., An empirical correction for absorption anisotropy. *Acta Cryst.* 1995, **A51**, 33-38.
58. Sheldrick, G. M. *Shelx-97 Programs for the Solution and Refinement of Crystal Structures*, University of Göttingen, Germany, 1997.
59. Speck, A. L., Single-crystal structure validation with the program PLATON. *J. Appl. Crystallogr.* 2003, **36**, 7-13.
60. McMurry, J., *Organic chemistry*. 4th ed.; Brooks/Cole Pub. Co.: Pacific Grove, 1996.

61. Tadeusz, L., Phosphonoacetic acid (H_3AP) and its salts $\text{KH}_2\text{AP} \cdot \text{H}_2\text{O}$, $(\text{NH}_4)\text{H}_2\text{AP}$, LiH_2AP , $\text{NaH}_2\text{AP} \cdot 2\text{H}_2\text{O}$, K_2HAP , $(\text{NH}_4)_2\text{HAP}$, $\text{Na}_2\text{HAP} \cdot 2\text{H}_2\text{O}$, $(\text{NH}_4)_3\text{AP} \cdot 2\text{H}_2\text{O}$ and $\text{Na}_3\text{AP} \cdot 10\text{H}_2\text{O}$. *Acta Cryst.* 1997, **C53**, 28-42.
62. *CCDC*, Version 5.29; November 2007.
63. Brown, I. D., On the geometry of $\text{O}-\text{H} \cdots \text{O}$ hydrogen bonding. *Acta Cryst.* 1976, **A32**, 24-31.
64. Hamilton, W. C., The structure of solids. *Annu. Rev. Phys. Chem.* 1962, **13**, 19-40.
65. Colthup, N. B.; Daly, L. H.; Wiberley, S. E., *Introduction to Infrared and Raman Spectroscopy*. 3rd ed.; Academic Press: New York, 1990.
66. Bratoz, S.; Hadzi, D.; Sheppard, N., The infra-red absorption bands associated with the COOH and COOD groups in dimeric carboxylic acid—II: the region from 3700 to 1500 cm^{-1} . *Spectrochim. Acta* 1956, **8**, 249-261.
67. Braunholtz, J. T.; E, H. G.; Mann, F. G.; Sheppard, N., Infrared spectra and hydrogen bonding in compounds containing $\text{X}(=\text{O})\text{OH}$ groups. *J. Chem. Soc.* 1959, 868-872.
68. Bardos, T. J.; Datta-Gupta, N.; Hebborn, P., Synthesis, chemistry, and preliminary pharmacology of arsenical nitrogen mustards and structurally related nonalkylating arsenicals. *J. Med. Chem.* 1966, **9**, 221-227.
69. Johnson, A. W., *Ylides and Imines of Phosphorus*. Wiley-Interscience: New York, 1993.
70. Jeffrey, G. A., Hydrogen-bonding: an update. *Cryst. Rev.* 2003, **9**, 135-176.
71. Grimme, S., Do special noncovalent π - π stacking interactions really exist? *Angew. Chem., Int. Ed. Engl.* 2008, **47**, 3430-3434.

72. Henderson, W.; Nicholson, B. K.; McCaffrey, L. J., Applications of electrospray mass spectrometry in organometallic chemistry. *Polyhedron* 1998, **17**, 4291-4313.
73. Cech, N. B.; Enke, C. G., Practical implications of some recent studies in electrospray ionization fundamentals. *Mass Spectrom. Rev.* 2001, **20**, 362-387.
74. Stothers, J. B.; Lauterbur, P. C., ¹³C Chemical shifts in organic carbonyl groups. *Can. J. Chem.* 1964, **42**, 1563-1576.
75. Breunig, H. J.; Rösler, R., New developments in the chemistry of organoantimony and -bismuth rings. *Chem. Soc. Rev.* 2000, **29**, 403-410.
76. Day, J. A.; Montes-Bayón, M.; Vonderheide, A. P.; Caruso, J. A., A study of method robustness for arsenic speciation in drinking water samples by anion exchange HPLC-ICP-MS. *Anal. Bioanal. Chem.* 2002, **373**, 664-668.
77. Londesborough, S.; Mattusch, J.; Wennrich, R., Separation of organic and inorganic arsenic species by HPLC-ICP-MS. *Fresenius. J. Anal. Chem.* 1999, **363**, 577-581.
78. Weast, R. C.; Astle, M. J., *CRC Handbook of Chemistry and Physics*. ? ed.; CRC Press, Inc.: Boca Raton, Florida, 1982.
79. Sands, D. E., The crystal structure of monoclinic (β) sulfur. *J. Am. Chem. Soc.* 1965, **87**, 1395-1396.
80. Templeton, L. K.; Templeton, D. H.; Zalkin, A., Crystal structure of monoclinic sulfur. *Inorg. Chem.* 1976, **15**, 1999-2991.
81. Goldsmith, L. M.; Strouse, C. E., Molecular dynamics in the solid state. The order-disorder transition of monoclinic sulfur. *J. Am. Chem. Soc.* 1977, **99**, 7580-7589.
82. Greenwood, N. N.; Earnshaw, A., *Chemistry of the Elements*. Pergamon Press: Oxford, England, 1989.

-
83. Cotton, F. A.; Wilkinson, G.; Murillo, C. A.; Bochmann, M., *Advanced Inorganic Chemistry*. 6th ed.; Wiley-Interscience: New York, 1999.